



# SKB rapport

## R-97-17

November 1997

On regional flow in Baltic Shield rock

An application of an analytical solution  
using hydrogeologic conditions at  
Aberg, Beberg and Ceberg of SR 97

---

*Göran Rehbinder, Dept. of Civil and Environmental Eng., KTH*

*Sven Follin, Golder Associates, Stockholm*

*Alf Isaksson, Dept. of Signals, Sensors and Systems, KTH*



SKB, Box 5864, 102 40 Stockholm  
Telefon 08-665 28 00 • Telefax 08-661 57 19 • Telex 13108 S

## **ON REGIONAL FLOW IN BALTIC SHIELD ROCK**

### **AN APPLICATION OF AN ANALYTICAL SOLUTION USING HYDROGEOLOGIC CONDITIONS AT ABERG, BEBERG AND CEBERG OF SR 97**

Göran Rehbinder<sup>1</sup>, Sven Follin<sup>2</sup>, Alf Isaksson<sup>3</sup>

- 1            Dept.of Civil and Environmental Engineering, KTH
- 2            Golder Associates, Stockholm
- 3            Dept. of Signals, Sensors and Systems, KTH

November 1997

This report concerns a study which was conducted for SKB. The conclusions and viewpoints presented in the report are those of the author(s) and do not necessarily coincide with those of the client.

# **ON REGIONAL FLOW IN BALTIC SHIELD ROCK**

AN APPLICATION OF AN ANALYTICAL SOLUTION  
USING HYDROGEOLOGIC CONDITIONS AT  
ABERG, BEBERG AND CEBERG OF SR 97

*Göran Rehbinder*

Dept of Civil and Environmental Engineering, KTH

*Sven Follin*

Golder Associates, Stockholm

*Alf Isaksson*

Dept of Signals, Sensors and Systems, KTH

November 10, 1997

## ABSTRACT

This report is one of many in support of SR 97, and is an analysis of the residence and transport times of a fluid particle at the three hypothetical domains of SR 97. The three domains are arbitrary named Aberg, Beberg and Ceberg. The report is intended to provide a quantitative assessment of the lateral length scales governing groundwater flow. The largest of these scales is believed to govern regional flow, i.e., flow at great depth. The calculated reference times presented in this report are fairly constant with the shortest reference time for Ceberg and the longest for Beberg. The difference in the calculated reference times are mainly due to the obtained differences in the lateral length scales at the three domains. However, the calculated residence times are extremely long. The corresponding transport times are very different from those obtained by means of numerical modeling of regional flow at Aberg, Beberg and Ceberg. The value is also contradicted by recent hydrochemical composition analyses of deep groundwater at Laxemar and Äspö. A speculative interpretation of this result is that large scale regional flow, in the sense of meaning flow paths with long lateral extent, should be questioned for the kind of depth (500 m) and hydrogeologic system (hard rock) dealt with in this report. In other words, large scale regional flow may play a role for a repository at great depth ( $\gg$  500 m), whereas non-periodic local variations in the topography may govern the flow pattern at moderate depths, e.g., depths less than 1000 m. There are several observations which support this interpretation.

## SAMMANFATTNING

Föreliggande rapport är utförd inom ramen för SR 97. Rapporten syftar till att kvantifiera vilka längdskalor som styr flödet på förvarsdjup vid Aberg, Beberg och Ceberg. Rapporten visar att de flödes- och transporttider som erhållits är tämligen platsberoende med de kortaste tiderna för Ceberg och de längsta för Beberg. Det mest intressanta resultatet är emellertid att tiderna är långa. Tiderna är mycket längre än vad som erhållits vid numerisk flödesmodellering och mycket längre än vad som erhållits vid tolkning av hydrokemiska data. En möjlig tolkning av det erhållna resultatet är att flödet i sprickigt berg på den studerade nivån 500 m inte påverkas av de längdskalor som identifierats (~200 km) utan av kortare längdskalor (lokala terrängförhållanden). Numerisk flödesmodellering och hydrokemiska data indikerar att denna möjlighet för närvarande inte kan uteslutas.

# CONTENTS

ABSTRACT

SAMMANFATTNING

<b>1 INTRODUCTION .....</b>	<b>2</b>
<b>1.1 BACKGROUND.....</b>	<b>2</b>
<b>1.2 PURPOSE AND SCOPE .....</b>	<b>4</b>
<b>1.3 THEORETICAL APPROACH, MAIN SOURCES OF         INFORMATION AND LAYOUT OF REPORT .....</b>	<b>4</b>
<b>2 THE RESIDENCE TIME OF A FLUID PARTICLE .....</b>	<b>5</b>
<b>3 TOPOGRAPHIC WAVE LENGTHS .....</b>	<b>11</b>
<b>3.1 ABERG.....</b>	<b>11</b>
<b>3.1.1 Transverse Aberg Domain.....</b>	<b>14</b>
<b>3.1.2 Longitudinal Aberg Domain .....</b>	<b>16</b>
<b>3.2 BEBERG .....</b>	<b>18</b>
<b>3.2.1 Total Beberg Domain .....</b>	<b>20</b>
<b>3.2.2 Eastern Half of the Beberg Domain .....</b>	<b>22</b>
<b>3.3 CEBERG .....</b>	<b>24</b>
<b>4 CONDUCTIVITY TRENDS.....</b>	<b>29</b>
<b>4.1 METHOD.....</b>	<b>29</b>
<b>4.2 ABERG.....</b>	<b>30</b>
<b>4.3 BEBERG .....</b>	<b>32</b>
<b>4.4 CEBERG .....</b>	<b>34</b>
<b>5 RESIDENCE TIMES .....</b>	<b>36</b>
<b>6 DISCUSSION AND CONCLUSIONS.....</b>	<b>38</b>
<b>7 REFERENCES .....</b>	<b>40</b>

## APPENDIX A

*DERIVATION OF THE RESIDENCE TIME FOR PERIODIC  
TOPOGRAPHY*

## APPENDIX B

*DERIVATION OF CHARACTERISTIC WAVE LENGTHS OF THE  
TOPOGRAPHY*

# 1 INTRODUCTION

## 1.1 BACKGROUND

Swedish Nuclear Fuel and Waste Management Company (SKB) is responsible for the safe handling and disposal of nuclear wastes in Sweden. This responsibility includes conducting studies into the siting of a deep repository for high-level nuclear waste. The safety report for 1997 (SR 97) will present a performance assessment (PA) of the overall safety of a deep repository at three hypothetical sites in Sweden. One component of these PA studies is hydrogeologic modeling to examine the possible transport of radionuclides from the emplacement waste packages through the host rock to the accessible environment.

The three hypothetical sites are arbitrarily named Aberg, Beberg and Ceberg, each of which is loosely associated to previous site characterization studies conducted by SKB. These are:

- Aberg, which is associated to the Äspö Hard Rock Laboratory in the eastern part of southern Sweden,
- Beberg, which is associated to a former study site called Finnsjön, in the southeastern part of central Sweden, and
- Ceberg, which is associated to a study site called Gideå, in southeastern part in northern Sweden.

The locations of Aberg, Beberg and Ceberg, as used in this study, are shown in Figure 1.1. It should be noted that in order to provide sufficient input information, the sizes of the domains are made much larger than the sizes of the original domains associated with the previous site characterization studies at Äspö HRL, Finnsjön and Gideå.

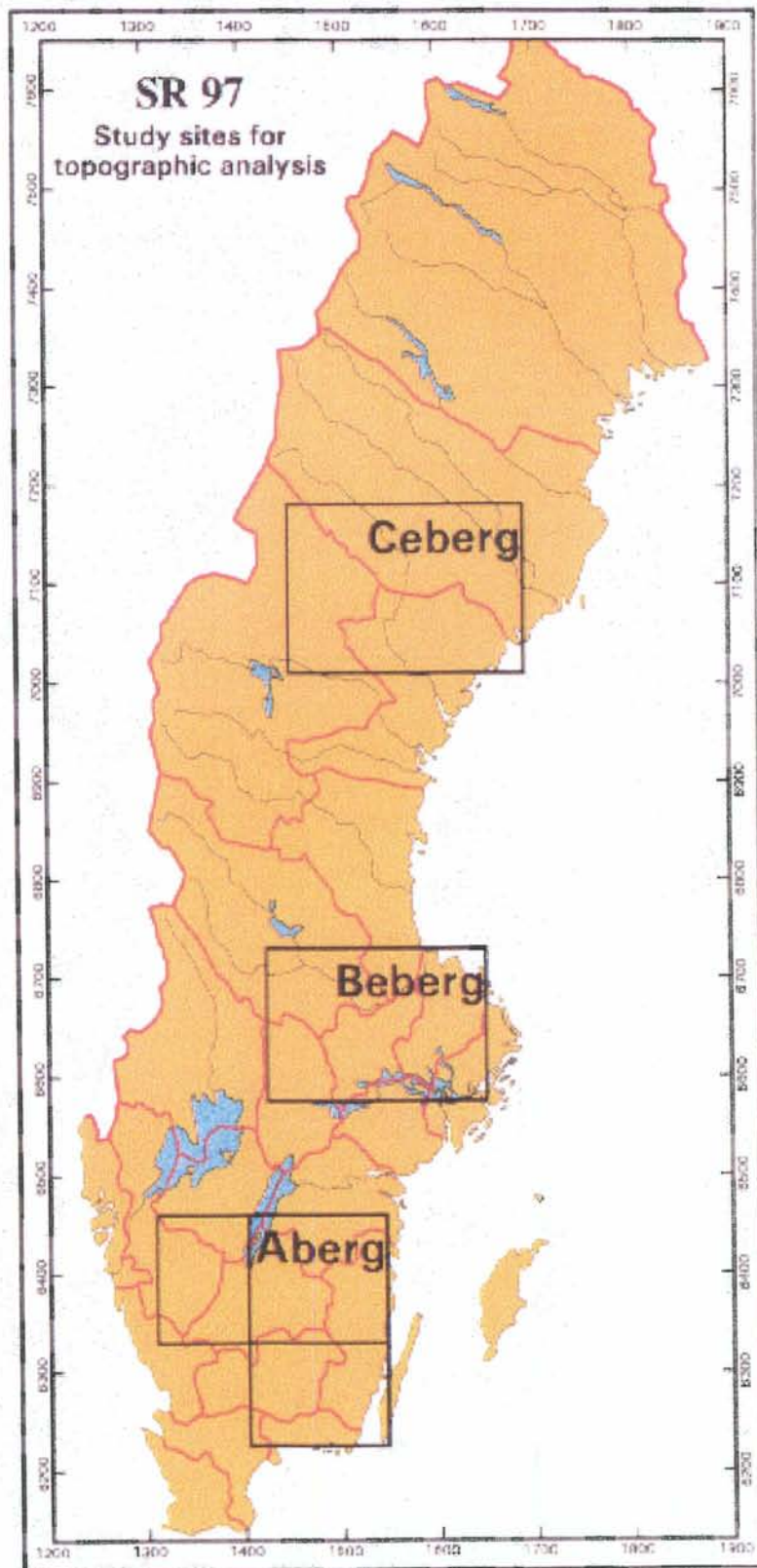


**Figure 1.1** Map over Sweden showing the locations and sizes of the three the hypothetical domains Aberg, Beberg and Ceberg.



## **1.2 PURPOSE AND SCOPE**

This report is one of many in support of SR 97, and is an analysis of the residence time of a fluid particle at the three hypothetical domains. The magnitude of the groundwater flux per unit area is determined by two factors. The first factor is the (hydraulic) conductivity of the rock mass. The other factor is the magnitude of the hydraulic gradient. The latter factor is composed of two parts, viz. the variations in the elevation of the phreatic surface (groundwater table) and the lateral length of the variations. This report is intended to provide a quantitative assessment of the lateral length scales governing groundwater flow. The largest of these scales is believed to govern regional flow, i.e., flow at great depth. Residence and transport times are then estimated for flow through a hypothetical repository at 500 m depth using domain specific length scales and conductivity values.

## **1.3 THEORETICAL APPROACH, MAIN SOURCES OF INFORMATION AND LAYOUT OF REPORT**

The approach used in this study was based on the derivation of the residence time for periodic topography by Rehbinder & Isaksson (1998). An excerpt from their work is presented in Appendix A of this report.

For the purpose of this study input to the closed solution was derived from the Swedish Topographic Data Base (topographic wave lengths) and the Well Archive at the Swedish Geological Survey (rock conductivity). The analysis of the topographic information is presented in Chapter 3 whereas the hydraulic analysis is presented in Chapter 4. In Chapter 5 the results of the analyses are inserted into the theoretical solution and domain specific residence and transport times are compiled. Chapter 6 contains a discussion and the conclusions of the present study.

## 2 THE RESIDENCE TIME OF A FLUID PARTICLE

The flow of the groundwater in an open aquifer or in the bedrock is induced by spatial variations of the level of the phreatic surface. The magnitude of the flux per unit area is determined by two factors. The most important one is the conductivity of the rockmass. The other factor is the magnitude of the hydraulic gradient. The latter factor is composed of two parts, viz. the variations in the level of the phreatic surface and the lateral length scale of the variations. The situation is sketched in figure 2.1, which shows the topography of a fictitious landscape.

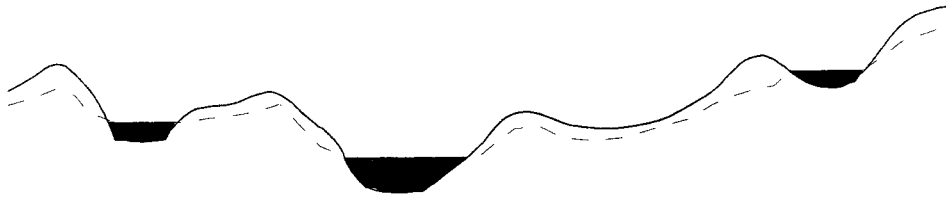


**Figure 2.1** A section of the topography of a fictitious landscape. The dashed line indicates the phreatic surface.

The absence of marked peaks is characteristic for the Fennoscandian shield, which has been subjected to several glaciations. If the lateral length scale is small, the hydraulic gradient is large, which means that the flux per unit area is large but concentrated to the vicinity of the ground surface. If, on the other hand, the length scale is large, the gradient is small, which means that the flux per unit area is small, but non-negligible at great depth. The shape of the phreatic surface is not characterized by *one* length scale, but by several. However, the largest of these governs the flow at great depth.

It is not immediately clear how large the governing lateral length scale is, or if there exists more than one *governing* length scale. The topography is two-dimensional rather than one-dimensional. The situation becomes even more complicated if the local inhomogeneity and anisotropy of the conductivity are significant. Any length scale that may govern the flow must be compared with other possible length scales of the problem. Thus the problem can be split in two parts:

### *1. Identification of the governing lateral length scales*

If the depth of the repository is large, the governing lateral length scale may be of continental size. Since the phreatic surface is two-dimensional, length scale in different directions may differ. A crucial question is how the characteristic lateral length scale can be measured with reasonable effort. It seems likely that the large lateral length scale of the phreatic surface corresponds to that of the topography. A fictitious phreatic surface, which corresponds to the fictitious topography, is sketched in Figure 2.1.

The largest length scale of the topography of Scandinavia is characterized by the Caledonian mountains. The ridge causes both the surface water and the groundwater to flow westward to the Atlantic and eastward to the Baltic. The elevation trend due to the mountain chain is one-dimensional but non-periodic, i.e., it can be treated as trend.

The topography is two-dimensional in general and has a structure that often appears complex. However, folding and faulting of the bedrock and loose sand and gravel structures of quaternian origin on top of the bed rock may cause topographic "waves". These can have characteristic directions and wavelengths, that cannot readily be seen on a map. The Swedish Topographic Data Base in digital form (GIS) can be used to identify possible topographic "waves".

The Swedish Topographic Data Base covers the entire country except for the great lakes in the southern part. The mesh is quadratic and the mesh size is 500 m. Thus, the database contains almost two million elevation figures.

## 2. *The large scale inhomogeneity of the conductivity of the bedrock*

The Fennoscandian shield appears to have at least one large scale hydraulic property. The hydraulic conductivity decreases with increasing depth. The spread of measured data is large, but it has been suggested that the conductivity decreases "logarithmically" with depth. The simplest representation of such a conductivity, which will be shown to be convenient from a calculational point of view, is

$$K(z) = K_0 e^{-z/z_0} \quad \text{m/s}$$

where the  $z$ -axis is directed *downwards* and  $z_0$  is a characteristic length. In the following, the velocity or the residence time of a fluid particle have *not* been adjusted for the effect of porosity.

The Well Archive at the Swedish Geological Survey can be used to identify possible conductivity trends at depth. The Well Archive covers large parts of Sweden, but the wells are generally shallow, e.g., less than 120 m and with a median around 60-70 m.

Consider a sinusoidal two-dimensional topography the wave length and elevation of which are  $L$  and  $\phi_0$ , respectively. The topography is flat, i.e.

$$L \gg \phi_0$$

Let an  $x$ -axis be at the ground level and a  $z$ -axis vertically *downwards* through the top of a ridge. A repository is placed at  $(x_r, z_r)$ , see Figure 2.2.

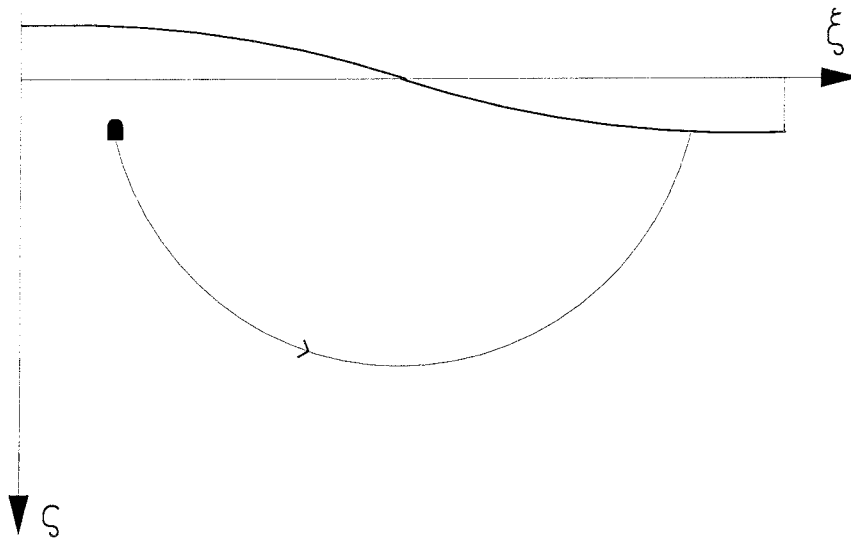


**Figure 2.2** A flat sinusoidal topography with a streamline from a repository to the free surface.

A fluid particle that is released from the repository will reach the free surface after the *residence time*  $T$ . A derivation of the streamlines and residence time is presented in appendix A.

In all practical cases

$$L \gg z_0$$

$$L \gg z_r$$

which implies that

$$T = \frac{L^2}{4\pi^2 \phi_0 K_0} \frac{\pi - x_r / L - \arcsin(e^{-z_r/z_0} \sin(2\pi x_r / L))}{e^{-z_r/z_0} \sin(2\pi x_r / L)}$$

The shortest residence time occurs if the repository is located below a valley, i.e.

$$\inf T = \frac{L^2}{4\pi^2 \phi_0 K_0} (e^{z_r/z_0} - 1) \quad x_r = \pi L$$

If the repository is located half way between a ridge and a valley, the residence time is

$$T = \frac{L^2}{4\pi^2 \phi_0 K_0} \frac{\pi/2 - \arcsin(e^{-z_r/z_0})}{e^{-z_r/z_0}} \quad x_r = \pi L / 2$$

Finally, if the repository is located below a ridge the residence time is

$$\sup T = \infty \quad x_r = 0$$

The problem of estimating the residence time is thus reduced to the problem of estimating  $L$ ,  $\phi_0$ ,  $K_0$  and  $z_0$ . As mentioned previously,  $L$  and  $\phi_0$  can be calculated from the elevation data base in GIS. Two different algorithms can be used. They are presented in Appendix B.

The residence time is practically determined by the *reference time*

$$T_{ref} = \frac{L^2}{4\pi^2 \phi_0 K_0},$$

which is independent of the location of the repository. It is obvious that if  $z_r \gg z_0$  or  $z_r \ll z_0$  the expressions above can be further simplified.

The above results, the derivation of which is presented in appendix A, are conservative for two reasons:

1. The estimated lateral length scale  $L$  is correct, whereas the estimated amplitude  $\phi_0$  is the amplitude of the *ground surface*, not the phreatic surface. This is sketched in Figure 2.1. This means that the driving hydraulic gradient

$$\nabla\phi < \phi_0 / L$$

2. If there is *no periodicity* but a single ridge, the estimates of the residence time above are underestimates. The reason is that if no valley exists, the point of outflow is located *far* from the ridge.

### **3 TOPOGRAPHIC WAVE LENGTHS**

As shown in Appendix B, the frequencies and wavelengths of the topographic relief can be identified from the elevation data base by means of Fast Fourier Transform and Autoregression. The Fast Fourier Transform is simpler and appears to be sufficient. Consequently, the below wavelengths have been identified exclusively by means of the Fast Fourier Transform.

#### **3.1 ABERG**

Due to the topography of southern Sweden the area around Aberg is divided in two domains, one transverse and one longitudinal, see Figures 3.1 and 3.2. The two domains are analyzed separately.



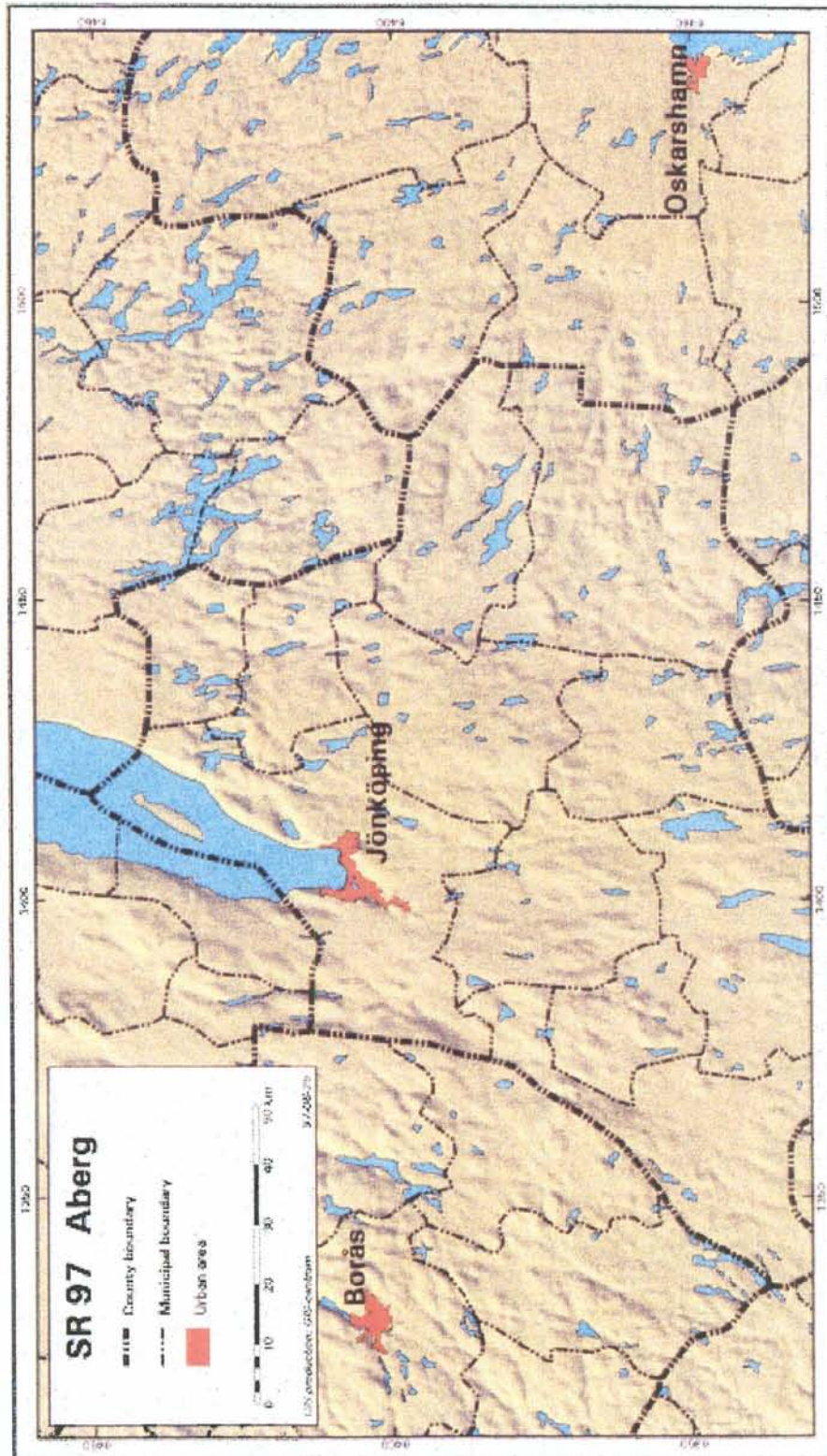
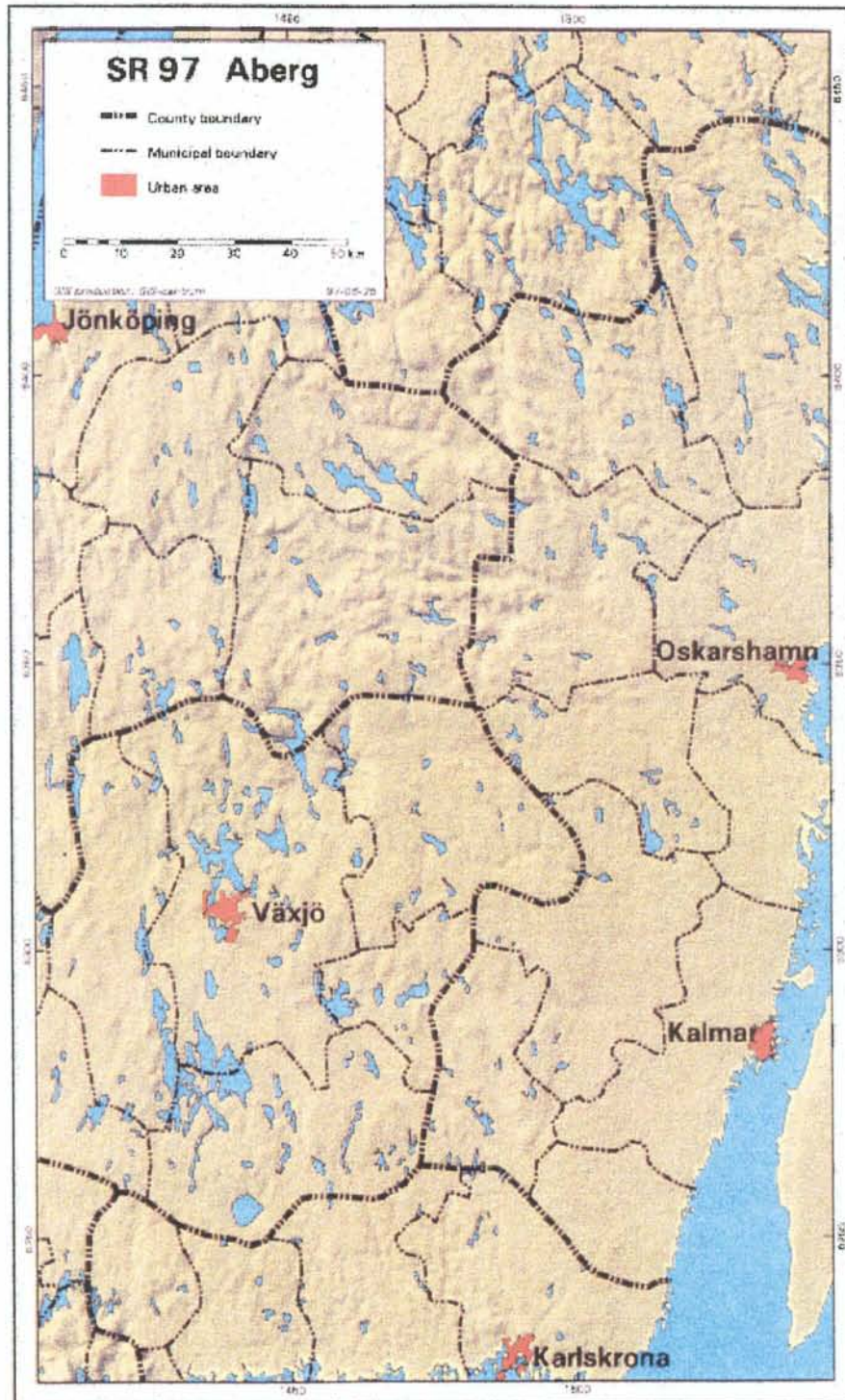


Figure 3.1 Topographic relief image of the transverse (W-E) Aberg domain.



**Figure 3.2** Topographic relief image of the longitudinal (N-S) Aberg domain.

### 3.1.1 Transverse Aberg Domain

The detrended topography is shown in Figure 3.3. The FFT-spectrum is shown in Figure 3.4.

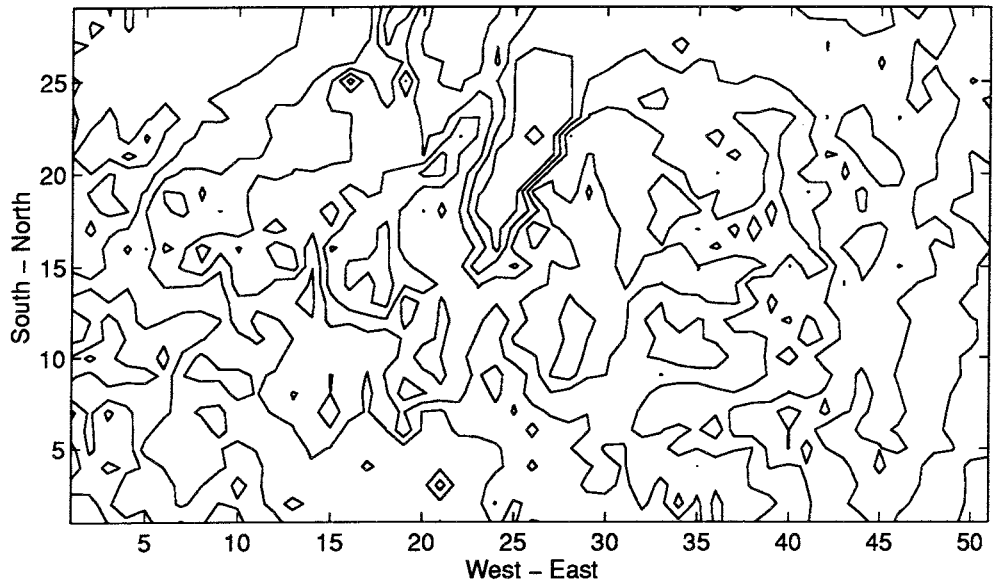


**Figure 3.3** The detrended topography of the transverse (W-E) Aberg domain. The numbers are in kilometers.

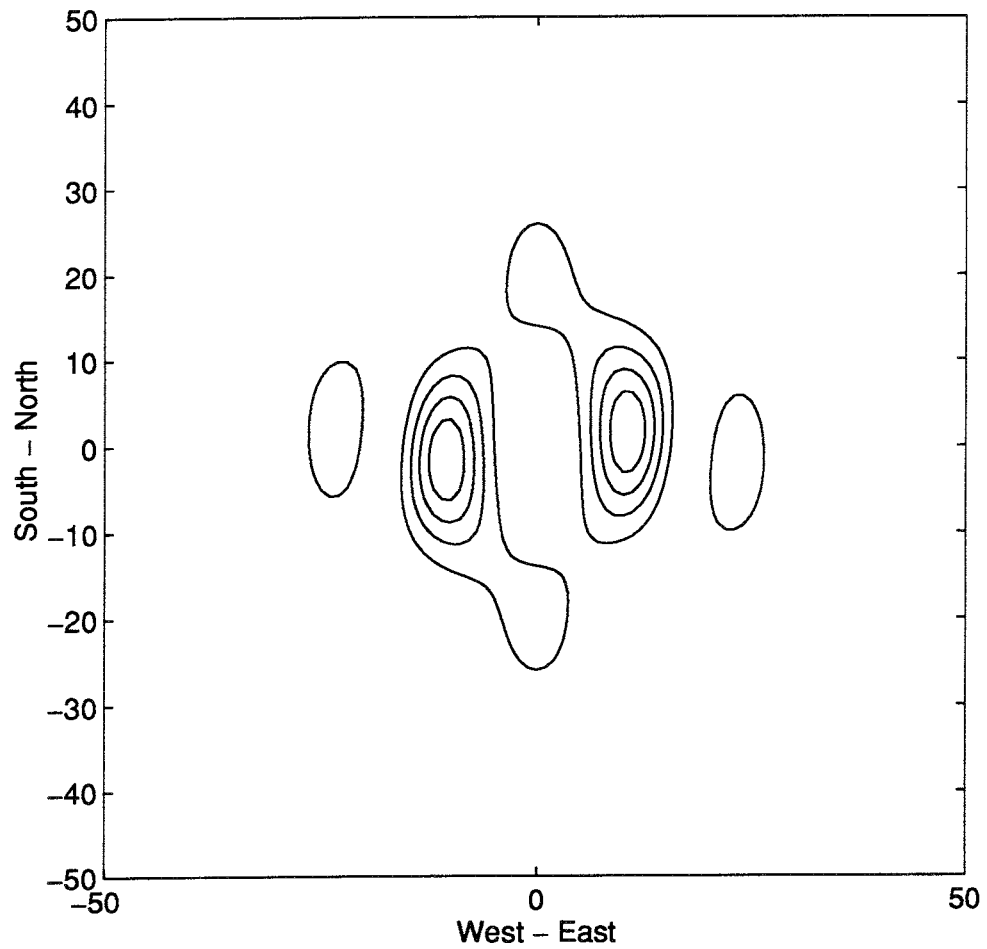


**Figure 3.4** The FFT-spectrum of the transverse (W-E) Aberg domain.

*One peak can be identified. Thus*

$$(n_1, n_2) = (2, 11)$$

which implies that the wavelength, the angle to the longitude and the amplitude are:

$$L = 229 \text{ km}$$

$$\theta = 10^\circ$$

$$\phi_0 = 67 \text{ m}$$

### 3.1.2 Longitudinal Aberg Domain

The detrended topography is shown in Figure 3.5. The FFT-spectrum is shown in Figure 3.6.

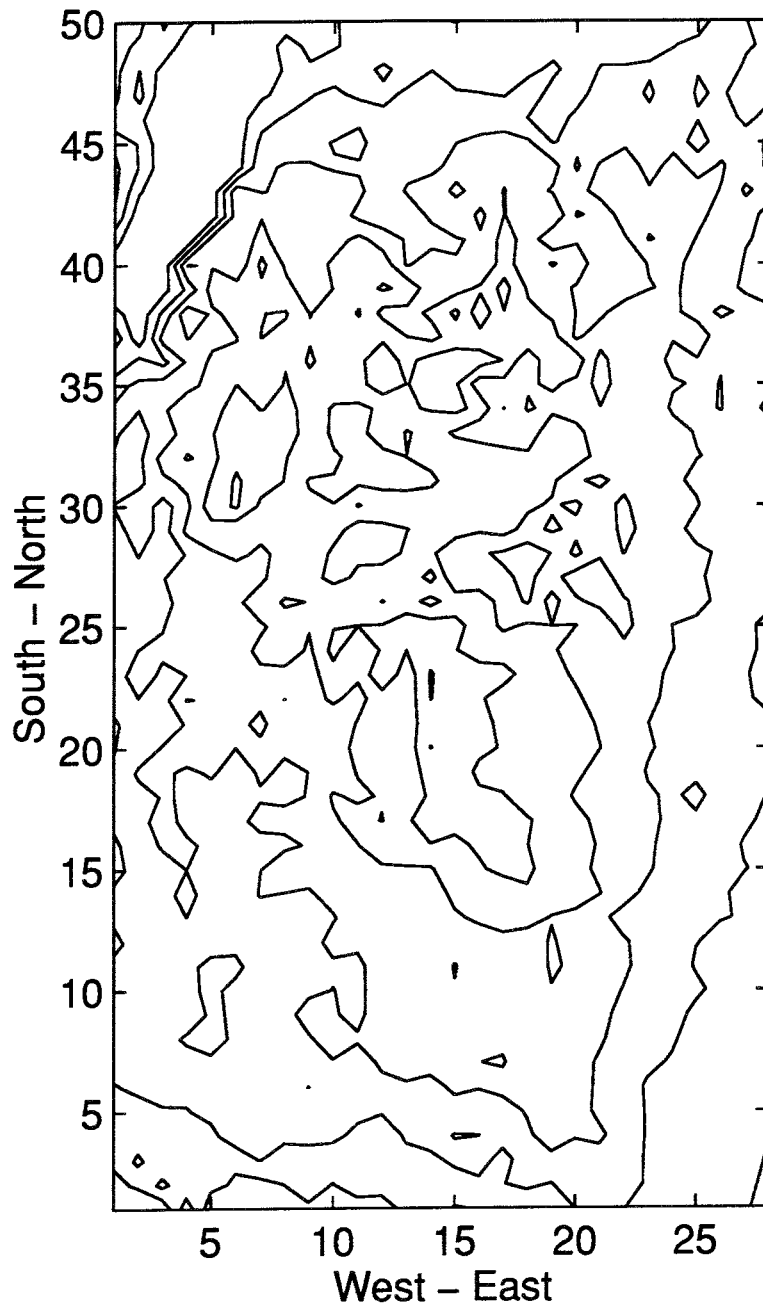


**Figure 3.5** The detrended topography of the longitudinal (N-S) Aberg domain.

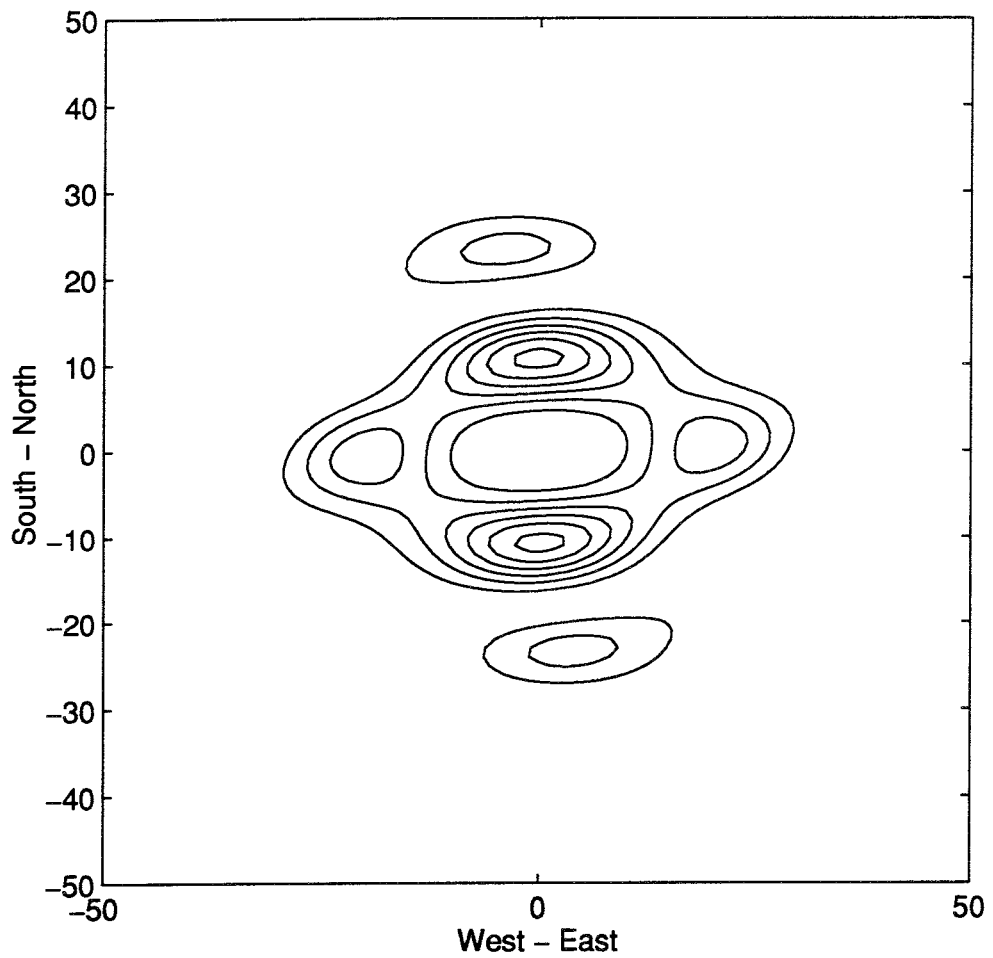


**Figure 3.6** The FFT-spectrum of the longitudinal (W-E) Aberg domain.

One peak can be identified. Thus,

$$(n_1, n_2) = (12, 1)$$

which implies that the wavelength, the angle to the longitude and the amplitude are:

$$L = 213 \text{ km}$$

$$\theta = 85^\circ$$

$$\phi_0 = 51 \text{ m}$$

The analyses show that there is not very much difference between the results apart from the orientation. As a matter of fact the patterns are almost perpendicular. This in combination with the identified wavelength ( $\sim 220$  km), which is comparable with the extent of half the domain, and amplitude ( $\sim 60$  m) indicate that the highland of southern Sweden is a circular hill.

## **3.2 BEBERG**

The domain, which is shown in Figure 3.7, is analyzed in two steps. First, the entire domain is analyzed and secondly the eastern half of the domain.

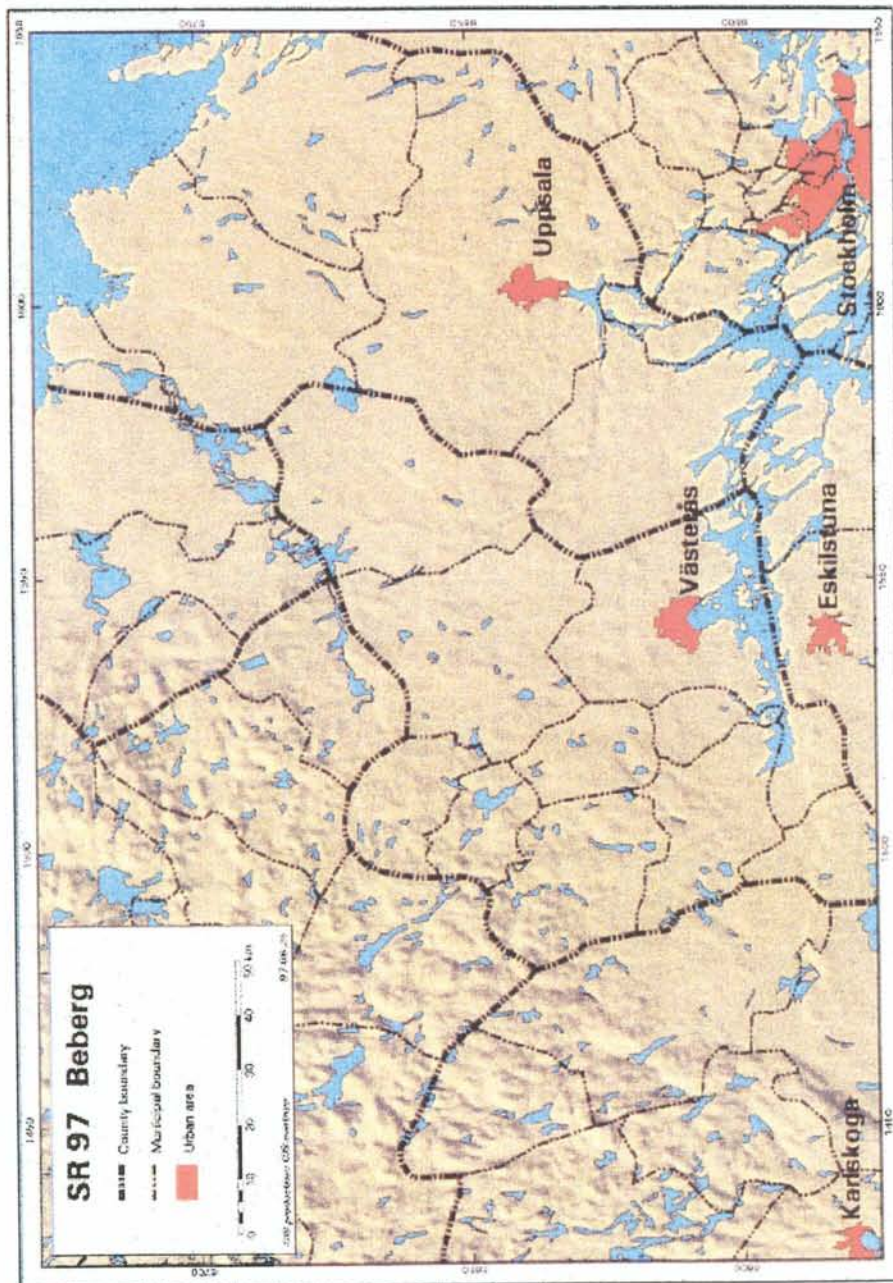
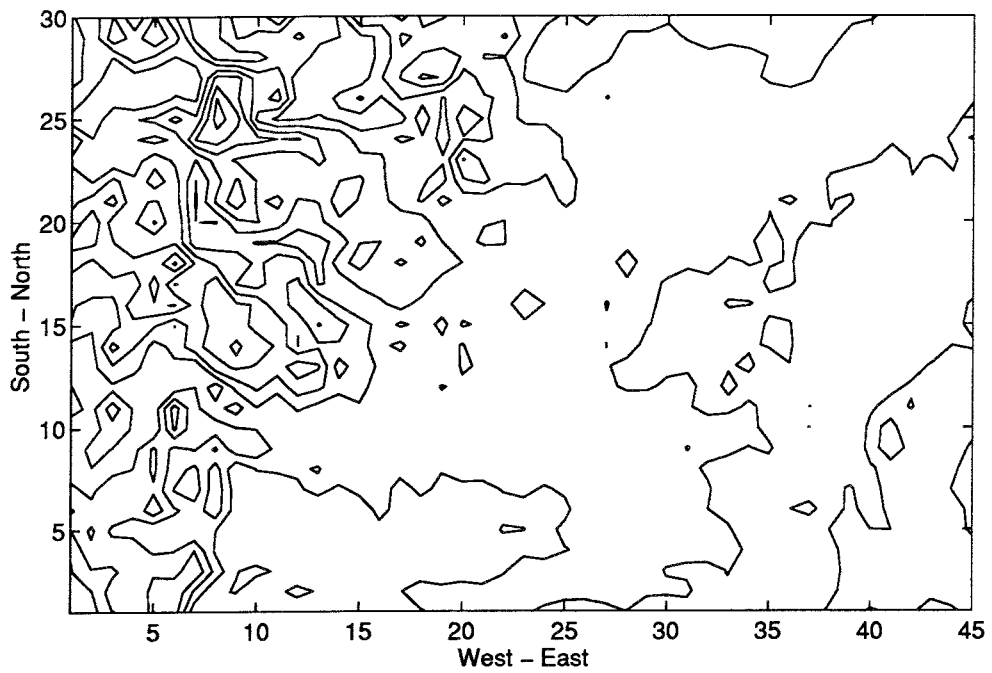


Figure 3.7 Topographic relief image of the Beberg domain.



### 3.2.1 Total Beberg Domain

The detrended topography is shown in Figure 3.8. The FFT-spectrum is shown in Figure 3.9.



**Figure 3.8** The detrended topography of the total Beberg domain. The numbers are in kilometres.

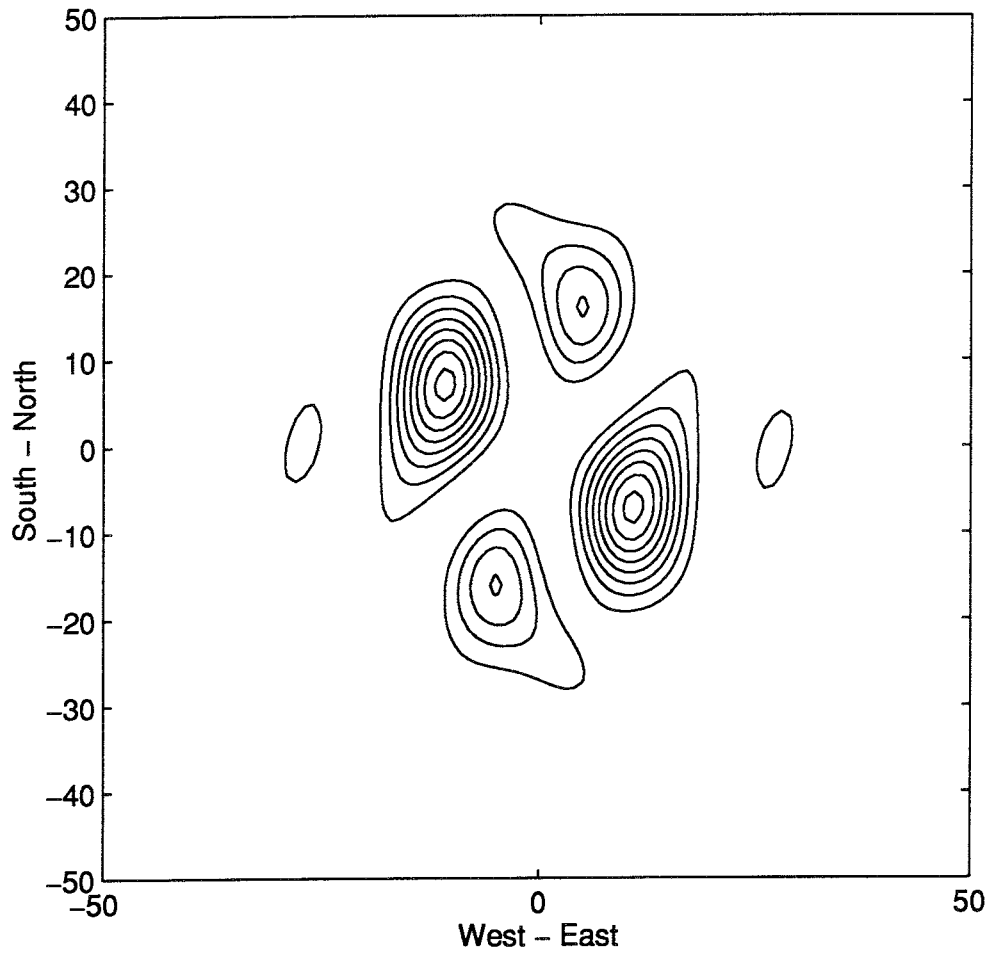


**Figure 3.9** The FFT-spectrum of the total Beberg domain.

Two peaks can be identified. Thus,

$$(n_1, n_2) = (-8, 10) \quad \text{and} \quad (n_1, n_2) = (15, 4)$$

which implies that the corresponding wavelength, angles to the longitude and the amplitudes are:

$$L = 200 \text{ km} \quad \text{and} \quad L = 165 \text{ km}$$

$$\theta = -39^\circ \quad \theta = 75^\circ$$

$$\phi_0 = 43 \text{ m} \quad \phi_0 = 30 \text{ m}$$

### 3.2.2 Eastern Half of the Beberg Domain

The detrended topography is shown in Figure 3.10.

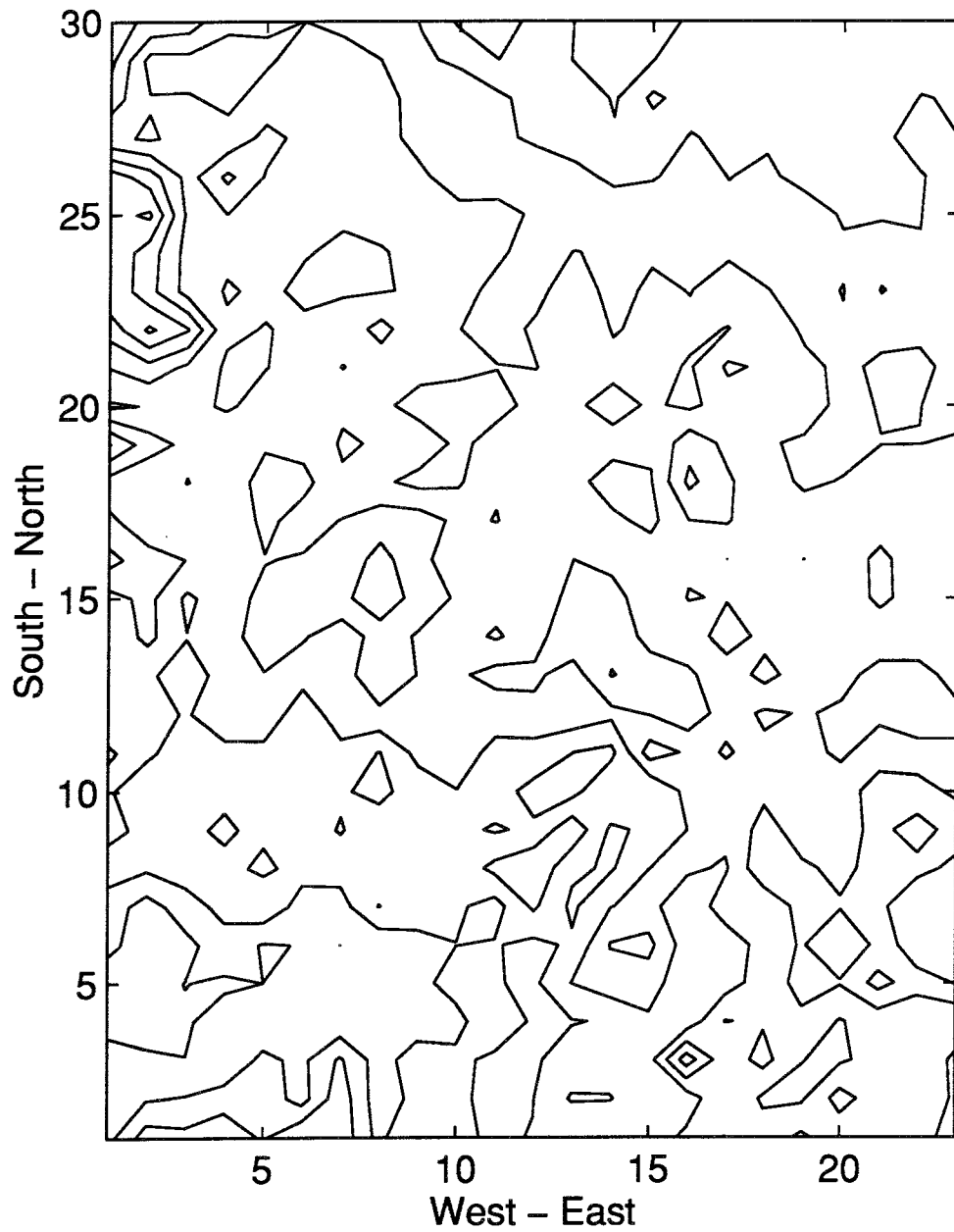


**Figure 3.10** The detrended topography of the eastern half of the Beberg domain. The numbers are in kilometres.

The FFT-spectrum is shown in Figure 3.11.

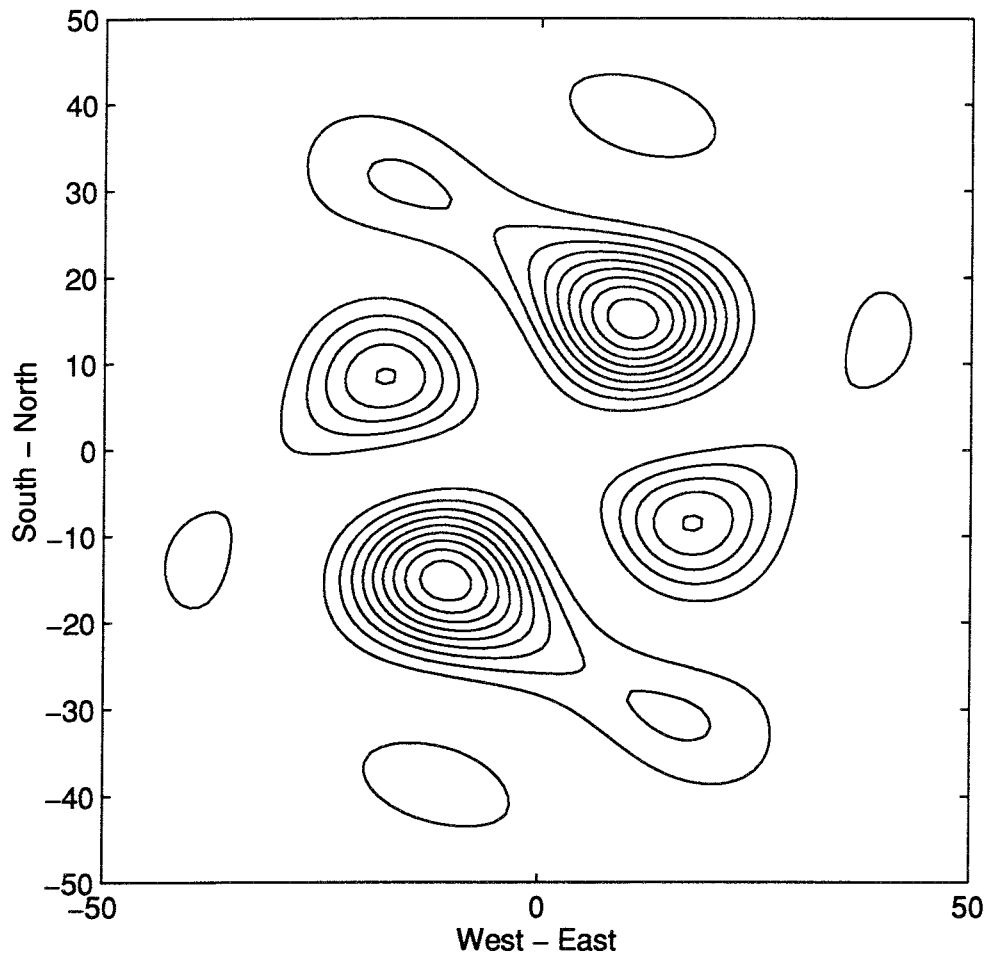


**Figure 3.11** The FFT-spectrum of the eastern half of the Beberg domain.

Two peaks can be identified. Thus,

$$(n_1, n_2) = (14, 10) \quad \text{and} \quad (n_1, n_2) = (-10, 17)$$

which implies that the corresponding wavelength, angles to the longitude and the amplitudes are:

$$\begin{array}{lll} L = 149 \text{ km} & \text{and} & L = 130 \text{ km} \\ \theta = 55^\circ & & \theta = -31^\circ \\ \phi_0 = 20 \text{ m} & & \phi_0 = 15 \text{ m} \end{array}$$

### **3.3 CEBERG**

The domain is shown in Figure 3.12 and the corresponding detrended topography in Figure 3.13. The FFT-spectrum is shown in Figure 3.14.

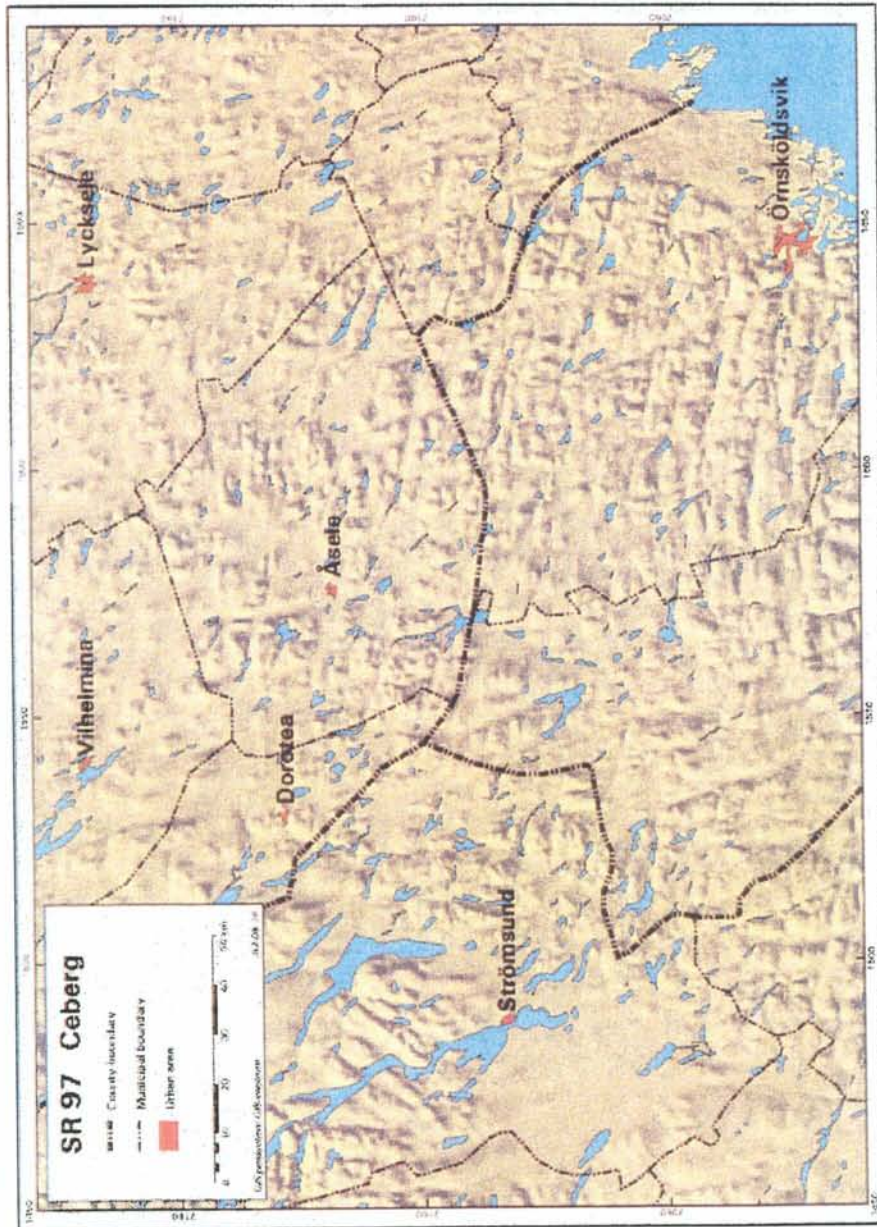
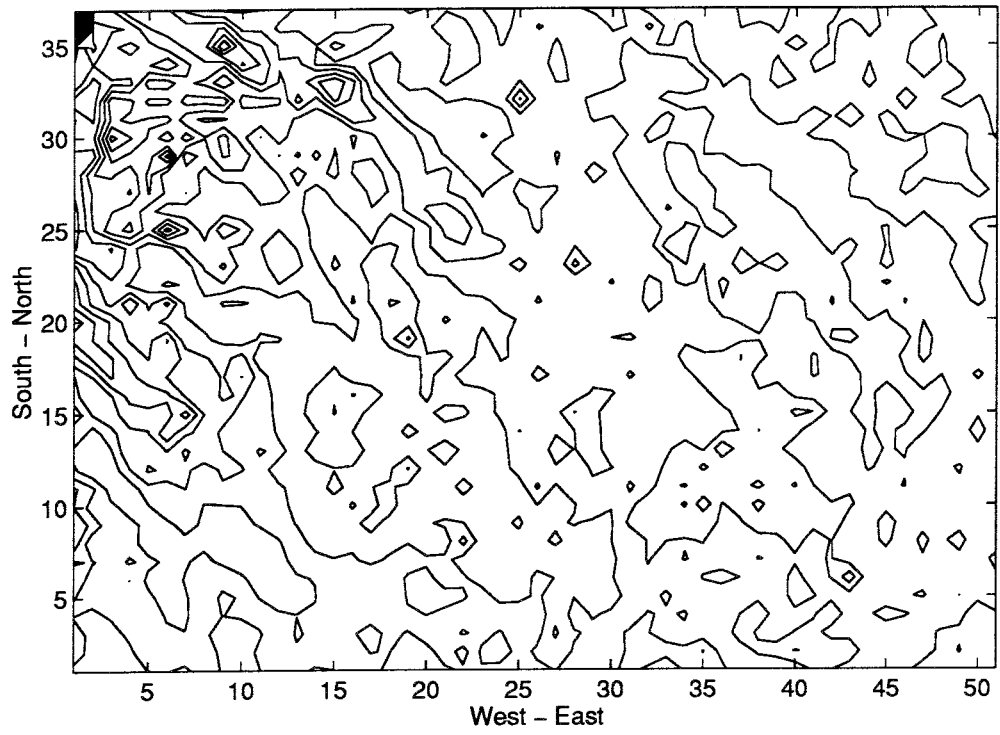
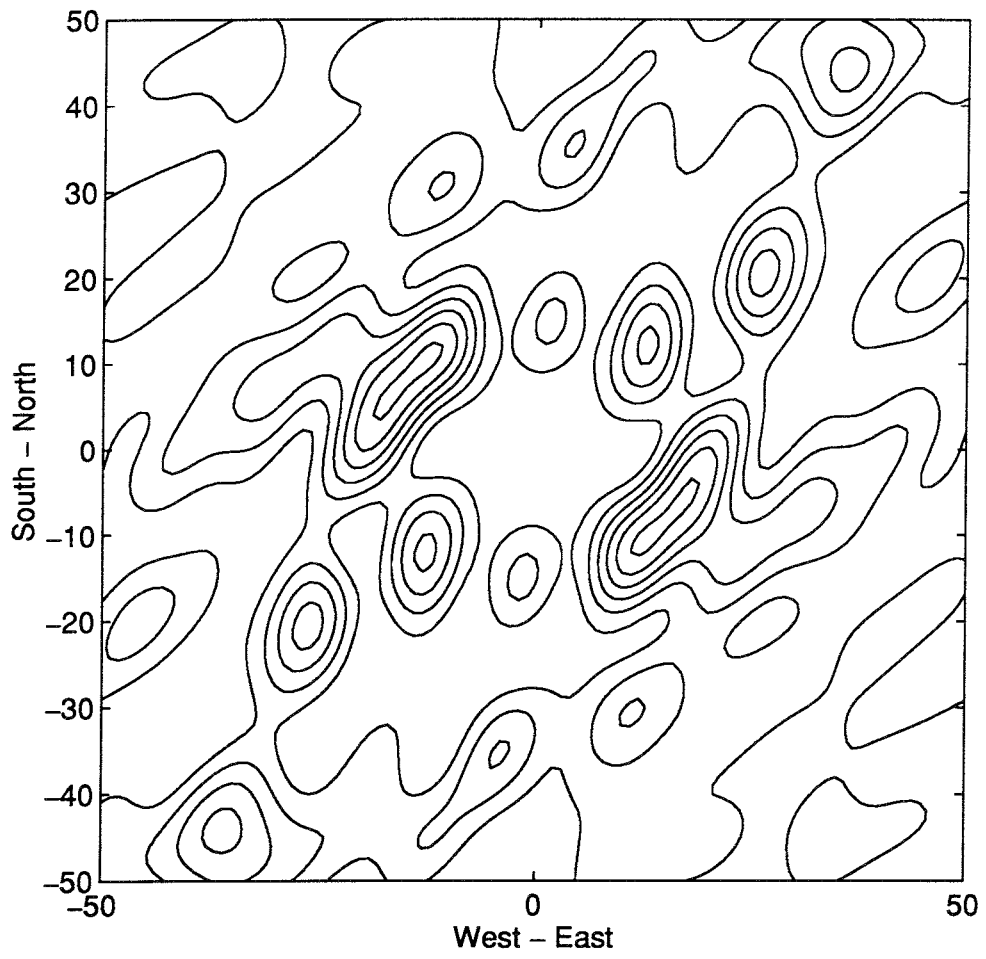


Figure 3.12 Topographic relief image of the Ceberg domain.



**Figure 3.13** The detrended topography of the Ceberg domain.



**Figure 3.14** The FFT-spectrum of the Ceberg domain.



Three peaks can be identified. Thus,

$$(n_1, n_2) = (-10, 13),$$

$$(n_1, n_2) = (19, 25)$$

and

$$(n_1, n_2) = (43, 35)$$

which implies that the corresponding wavelength, angles to the longitude and the amplitude are:

$$L = 156 \text{ km}$$

$$\theta = -38^\circ$$

$$\phi_0 = 59 \text{ m}$$

and

$$L = 82 \text{ km}$$

$$\theta = 37^\circ$$

$$\phi_0 = 50 \text{ m}$$

and

$$L = 46 \text{ km}$$

$$\theta = 51^\circ$$

$$\phi_0 = 49 \text{ m}$$

## 4 CONDUCTIVITY TRENDS

### 4.1 METHOD

The Well Archive at the Swedish Geological Survey contains geologic and hydrogeologic information from groundwater investigations and water well drillings in Sweden. The database is large and contains information from a long period of time. The quality of the information in the database has many limitations, however, a favorable aspect is that it covers many parts of Sweden.

Compared to the depth of a radwaste repository ( $\sim 500$  m) most wells in the Well Archive are shallow ( $\sim 60 - 70$  m). For those wells in the Well Archive where there exist records about the yield ( $Q$ , m<sup>3</sup>/s), the drawdown ( $s$ , m) and the length (depth) of the well drilled in rock ( $L$ , m), an apparent hydraulic conductivity ( $K$ , m/s) of the rock can be calculated from the formula

$$K = C(Q/s) / L$$

This formula is based on Thiem's equation for steady-state flow and Darcy's law for flow through porous media.  $C$  is geometrical factor which may be treated as a constant. A plot of  $K$  versus  $z = (L/2)$  is one means of studying if there is a depth trend in  $K$  towards depth. Two common trend (regression) equations in the literature are:

$$K(z) = K_0 e^{-z/z_0} \quad (\text{exponential trend})$$

$$K(z) = A / z^b \quad (\text{power trend})$$

## 4.2 ABERG

The location of Aberg, as defined in this study, is shown in Figure 1.1. Figures 3.1 and 3.2 show two topographic relief images of Aberg. For the purpose of this project, we have chosen three municipalities within the Aberg domain. These are Nässjö, Oskarshamn and Växjö. The information gathered in the Well Archive for these three municipalities have been used to estimate  $K = K(z)$  according to the two aforementioned trend formulae.

Figure 4.1 shows an example of a depth plot for Aberg. Table 4.1 shows that the exponential trend formula yields a useful value of  $K(0) = K_0$  whereas the power trend formula yields a more realistic value of  $K(500)$ . Thus, the final desired parameter,  $z_0$ , is back calculated using these two values of  $K$ .

**Table 4.1 Trend parameters for the Aberg domain.**

$K(z) = K_0 e^{-z/z_0}$ (exponential trend)					
Municipality	# of Wells	$r^2$ , %	$K_0$ , m/s	$z_0$ , m	$K(500)$ , m/s
Nässjö	407	52	1.10E-6	12.68	8.34E-24
Oskarshamn	685	53	1.07E-6	11.66	2.52E-25
Växjö	642	34	5.08E-7	19.53	3.69E-18
<u>Geom. mean</u>			<u>8.42E-7</u>		
$K(z) = A / z^b$ (power trend)					
Municipality	# of Wells	$r^2$ , %	A	b	$K(500)$ , m/s
Nässjö	407	53	2.31E-4	2.39	8.43E-11
Oskarshamn	685	58	4.83E-4	2.66	3.12E-11
Växjö	642	38	2.86E-5	1.71	6.82E-10
<u>Geom. mean</u>					<u>1.22E-10</u>
<i>Chosen Parameters</i>					
$K(z) = K_0 e^{-z/z_0}$ (exponential trend)					
	# of Wells	$r^2$ , %	$K_0$ , m/s	$z_0$ , m	$K(500)$ , m/s
ABERG	"2"	100	<u>8.42E-7</u>	56.54	<u>1.22E-10</u>

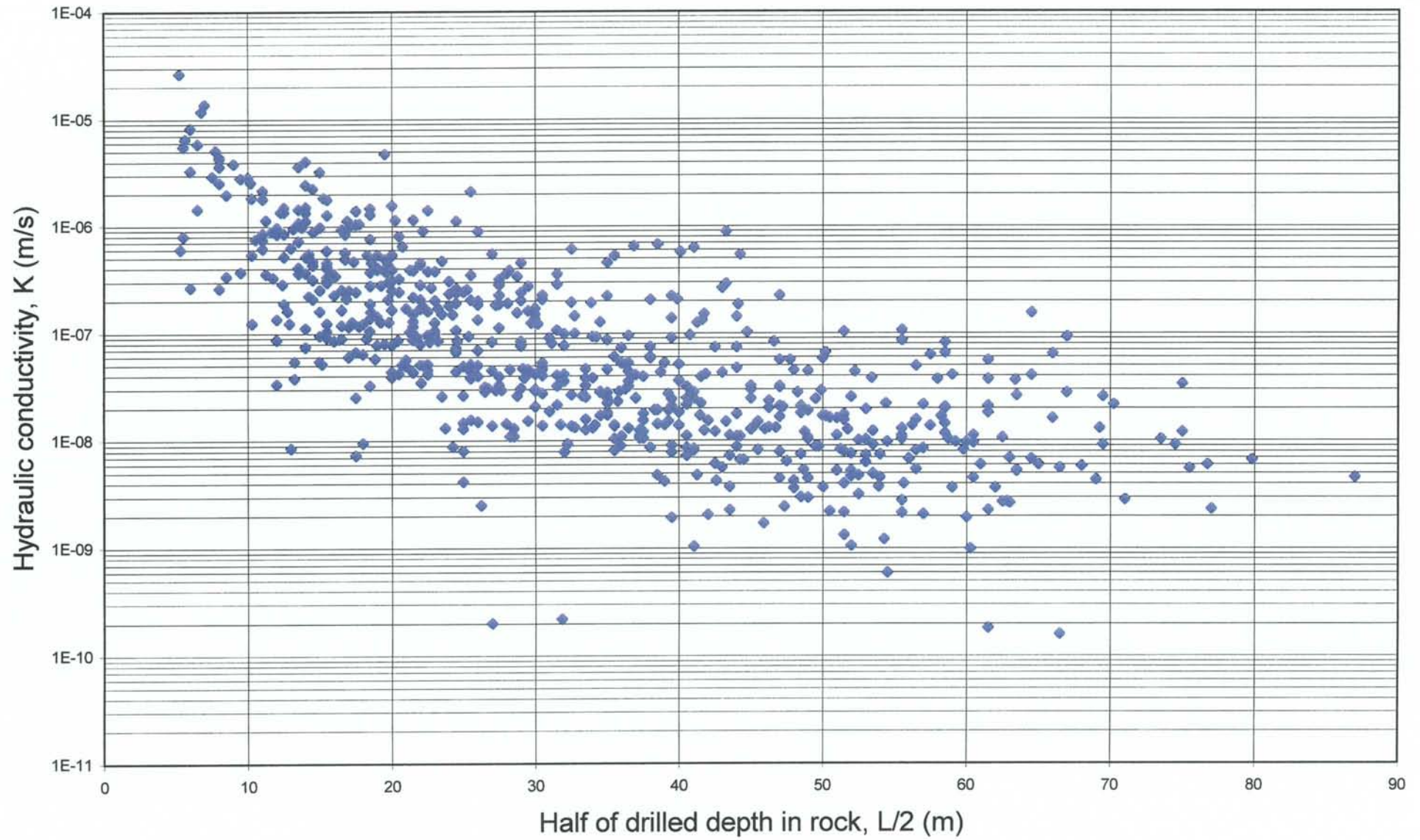


Figure 4.1 Cross plot of K versus L/2 for all SGU wells in Oskarshamn's municipality.

### 4.3 BEBERG

The location of Beberg, as defined in this study, is shown in Figure 1.1. Figure 3.7 shows a topographic relief image of Beberg. For the purpose of this project, we have chosen three municipalities within the Beberg domain. These are Avesta, Västerås and Östhammar. The information gathered in the Well Archive for these three municipalities have been used to estimate  $K = K(z)$  according to the two aforementioned trend formulae.

Figure 4.2 shows an example of a depth plot for Beberg. Table 4.2 shows that the exponential trend formula yields a useful value of  $K(0) = K_0$  whereas the power trend formula yields a more realistic value of  $K(500)$ . The desired parameter,  $z_0$ , is back calculated using these two values of  $K$ .

**Table 4.2 Trend parameters for the Beberg domain.**

$K(z) = K_0 e^{-z/z_0}$ (exponential trend)					
Municipality	# of Wells	$r^2$ , %	$K_0$ , m/s	$z_0$ , m	$K(500)$ , m/s
Avesta	448	65	1.14E-6	11.17	4.09E-26
Västerås	1252	45	1.00E-6	10.65	4.14E-27
Östhammar	1448	49	8.43E-7	10.63	3.15E-27
<u>Geom. mean</u>			<u>9.87E-7</u>		

$K(z) = A / z^b$ (power trend)					
Municipality	# of Wells	$r^2$ , %	A	b	$K(500)$ , m/s
Avesta	448	69	3.96E-4	2.63	3.15E-11
Västerås	1252	50	4.33E-4	2.69	2.33E-11
Östhammar	1448	53	2.81E-5	2.63	2.22E-10
<u>Geom. mean</u>					<u>2.54E-11</u>

#### *Chosen Parameters*

$K(z) = K_0 e^{-z/z_0}$ (exponential trend)					
	# of Wells	$r^2$ , %	$K_0$ , m/s	$z_0$ , m	$K(500)$ , m/s
<b>BEBERG</b>	"2"	100	<u>9.87E-7</u>	47.31	<u>2.54E-11</u>

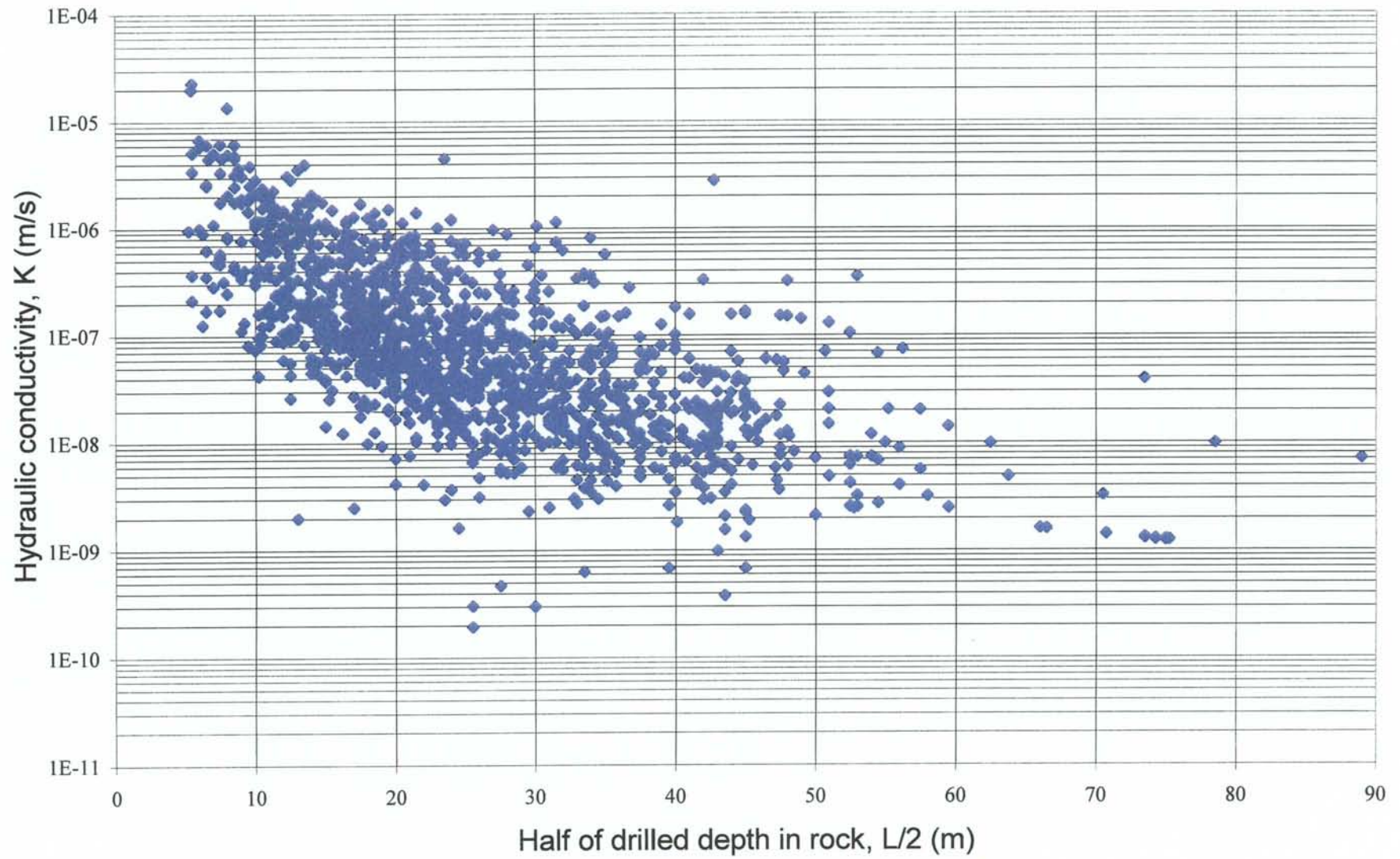


Figure 4.2 Cross plot of K versus L/2 for all SGU wells in Östhammar's municipality.

## 4.4 CEBERG

The location of Ceberg, as defined in this study, is shown in Figure 1.1. Figure 3.12 shows a topographic relief image of Ceberg. For the purpose of this project, we have chosen three municipalities within the Ceberg domain. These are Nordmaling, Åsele and Örnsköldsvik. The information gathered in the Well Archive for these three municipalities have been used to estimate  $K = K(z)$  according to the two aforementioned trend formulae.

Figure 4.3 shows an example of a depth plot for Ceberg. Table 4.3 shows that the exponential trend formula yields a useful value of  $K(0) = K_0$  whereas the power trend formula yields a more realistic value of  $K(500)$ . The desired parameter,  $z_0$ , is back calculated using these two values of  $K$ .

**Table 4.3 Trend parameters for the Ceberg domain.**

$K(z) = K_0 e^{-z/z_0}$ (exponential trend)					
Municipality	# of Wells	$r^2$ , %	$K_0$ , m/s	$z_0$ , m	$K(500)$ , m/s
Nordmaling	299	24	3.54E-7	22.14	5.49E-17
Åselen	58	39	1.55E-6	11.12	4.65E-26
Örnsköldsvik	1216	38	4.34E-7	16.90	6.18E-20
<u>Geom. mean</u>			<u>6.20E-7</u>		

$K(z) = A / z^b$ (power trend)					
Municipality	# of Wells	$r^2$ , %	A	b	$K(500)$ , m/s
Nordmaling	299	31	3.05E-4	1.76	5.59E-10
Åselen	58	41	1.44E-4	2.21	1.61E-10
Örnsköldsvik	1216	41	7.15E-5	2.21	7.80E-11
<u>Geom. mean</u>					<u>1.91E-10</u>

### *Chosen Parameters*

$K(z) = K_0 e^{-z/z_0}$ (exponential trend)					
	# of Wells	$r^2$ , %	$K_0$ , m/s	$z_0$ , m	$K(500)$ , m/s
CEBERG	"2"	100	<u>6.20E-7</u>	61.86	<u>1.91E-10</u>

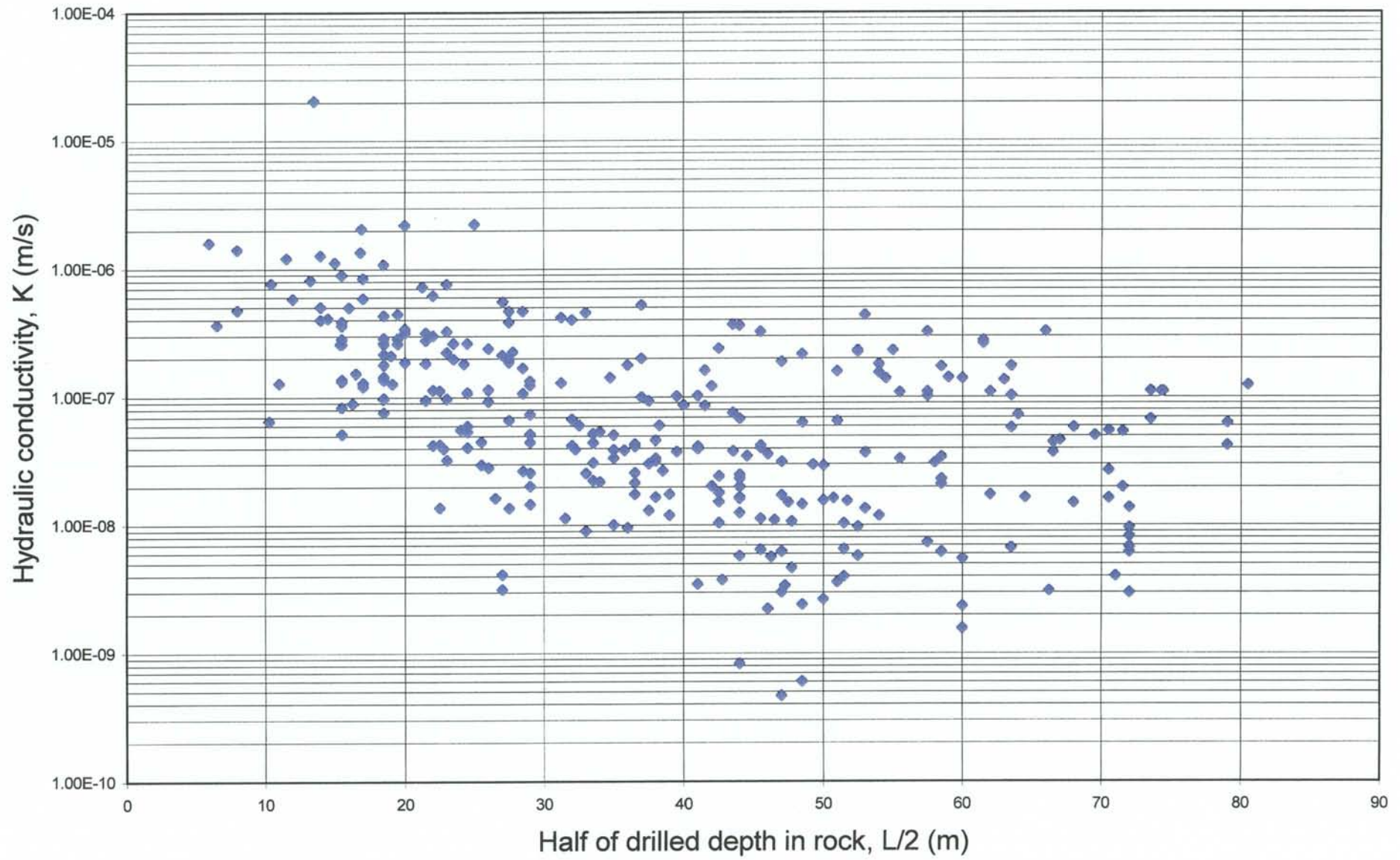


Figure 4.3 Cross plot of K versus L/2 for all SGU wells in Nordmaling's municipality.



## 5 RESIDENCE TIMES

The figures that have been produced from the elevation data and well yield data can now be used to estimate the residence time. As mentioned previously, the reference time is the governing parameter. The values yield:

### Aberg

$n$	$L$ km	$\phi_0$ m	$K_0$ m/s	$z_0$ m	$T_{ref}$ s
1	220	60	$8.4 \cdot 10^{-7}$	56	$7.7 \cdot 10^5$

### Beberg (The total domain)

$n$	$L$ km	$\phi_0$ m	$K_0$ m/s	$z_0$ m	$T_{ref}$ s
1	200	43	$9.9 \cdot 10^{-7}$	47	$7.6 \cdot 10^5$

### Beberg (The eastern half)

$n$	$L$ km	$\phi_0$ m	$K_0$ m/s	$z_0$ m	$T_{ref}$ s
1	149	20	$9.9 \cdot 10^{-7}$	47	$9.1 \cdot 10^5$
2	130	15	$9.9 \cdot 10^{-7}$	47	$9.2 \cdot 10^5$

### Ceberg

$n$	$L$ km	$\phi_0$ m	$K_0$ m/s	$z_0$ m	$T_{ref}$ s
1	156	59	$6.2 \cdot 10^{-7}$	62	$5.4 \cdot 10^5$
2	82	50	$6.2 \cdot 10^{-7}$	62	$1.7 \cdot 10^5$
3	46	49	$6.2 \cdot 10^{-7}$	62	$5.6 \cdot 10^4$

The conductivity decreases rapidly with the depth, in the sense that

$$z_r \gg z_0$$

This simplifies the expression of the residence time. Thus,

$$T = \begin{cases} T_{ref} \cdot e^{z_r/z_0} & x_r = \pi L & \text{repository below a valley} \\ T_{ref} \cdot \frac{\pi}{2} e^{z_r/z_0} & x_r = \pi L / 2 & \text{repository between a ridge and a valley} \\ \infty & x_r = 0 & \text{repository below a ridge} \end{cases}$$

Since the factor  $\pi/2 \sim 1$ ,

$$T > T_{ref} e^{z_r/z_0} \quad z_r \gg z_0$$

Obviously the depth of the repository and the reference time determine the residence time.

The reference time is fairly constant with the shortest reference time for Ceberg and the longest for Beberg. If the geometric mean of the reference times and  $z_0$  in Tables 4.1-4.3 are used, the residence time for a fluid particle leaving a repository at 500 m depth is approximately

$$T_{res} = 425 \cdot 10^3 \cdot e^{500/55} \text{ years} \approx 4 \cdot 10^9 \text{ years}$$

If the transport porosity of the rock is taken into account, e.g.,  $10^{-4}$ , the corresponding transport time of a fluid particle becomes  $4 \cdot 10^5$  years.

## 6 DISCUSSION AND CONCLUSIONS

The above analysis can be discussed and also questioned on several points. The following points deserve a particular discussion:

### 1. *The conductivity data*

The analysis of the well archive is impaired by considerable uncertainty. The data is extrapolated to a greater depth than could be recommended and the spread is large. However, if the "decay factor"  $z_0 \equiv 0$ , which means that there is no decrease in  $K$  towards depth, the analysis in appendix A shows that  $T \geq T_{ref}$ . In conclusion, the calculated values of  $T_{ref}$ , which are made for a small trend, are most likely conservative with regards to the nature of  $K$ .

It is necessary to keep in mind that the uncertainty in  $K$  is *not* associated with the simple analysis, but will appear no matter how elaborate a computer code may be. However, it is not clear if the conductivities are related to the flow per unit area in the ground or to the flow in cracks, i.e. to the pore velocity. This study assumes the former.

### 2. *The driving hydraulic gradient*

The driving hydraulic gradient is derived exclusively from the elevation data base, since

$$\nabla\phi \cong \frac{\phi_0}{L}$$

If the repository is located under a hilly *irregular* landscape, the driving hydraulic gradient cannot be identified by frequency analysis. Notwithstanding, the reference time is proportional to the *square* of the wave length and inversely proportional to the amplitude. In the case of a hilly *irregular* landscape, the lateral length scales are identified by mere

inspection of a map of the site, and the problem is solved with the aid of an elaborate computer code that assumes neither linearization of the boundary condition nor simple variation of the conductivity.

The calculated reference times presented in this report are fairly constant with the shortest reference time for Ceberg and the longest for Beberg. The difference in the calculated reference times are mainly due to the obtained differences in the lateral length scales (wavelengths) at the three domains. The calculated residence times are extremely long. For example, if the geometric mean of the reference times and  $z_0$  in Tables 4.1-4.3 are used, the residence time for a fluid particle leaving a repository at 500 m depth is approximately

$$T_{res} = 425 \cdot 10^3 \cdot e^{500/55} \text{ years} \approx 4 \cdot 10^9 \text{ years}$$

Now, if the transport porosity of the rock is taken into account, e.g.,  $10^{-4}$ , the corresponding transport time of a fluid particle becomes  $4 \cdot 10^5$  years.

This value is *very* different from the transport times obtained by means of numerical modeling of regional flow at Aberg (Svensson, 1997), Beberg (Hartley *et al.*, *in press*) and Ceberg (Boghammar *et al.*, *in press*). The value is also contradicted by recent hydrochemical composition analyses of deep groundwater at Laxemar and Äspö (see, e.g., Smellie and Laaksoharju, 1992; Laaksoharju *et al.*, 1995). A speculative interpretation of this result is that large scale regional flow, in the sense of meaning flow paths with long lateral extent, should be questioned for the kind of depth (500 m) and hydrogeologic system (hard rock) dealt with in this report. In other words, large scale regional flow may play a role for a repository at great depth ( $\gg 500$  m), whereas non-periodic local variations in the topography may govern the flow pattern at moderate depths, e.g., depths less than 1000 m. There are several observations which support this interpretation.

## 7 REFERENCES

Boghammar, A., B. Grundfelt and L. Hartley (*in press*) Investigation of the large scale regional hydrogeological situation at Ceberg, Report submitted to SKB, Swedish Nuclear Fuel and Waste Management Company, Stockholm.

Brigham, E. O. (1988) *The Fast Fourier Transform and its Applications*, Prentice Hall, Englewood Cliffs, NJ.

Hartley, L., A. Boghammar and B. Grundfelt (*in press*) Investigation of the large scale regional hydrogeological situation at Beberg, Report submitted to SKB, Swedish Nuclear Fuel and Waste Management Company, Stockholm.

Laaksoharju, M., J. Smellie, A.-C. Nilsson and C. Skårman (1995) Groundwater sampling and chemical characterisation of the Laxemar deep borehole KLX02, SKB TR 95-05, Swedish Nuclear Fuel and Waste Management Company, Stockholm.

Rehbinder, G. and A. Isaksson (1998) Large-scale flow of groundwater in Swedish bedrock. An analytical calculation, *Advances in Water Resources*, *in press*.

Smellie, J. and M. Laaksoharju (1992) *The Äspö Hard Rock Laboratory: Final evaluation of the hydrogeochemical pre-investigations in relation to existing geologic and hydraulic conditions*, SKB TR 92-31, Swedish Nuclear Fuel and Waste Management Company, Stockholm.

Svensson, U. (1997) A regional analysis of groundwater flow and salinity distribution in the Äspö area, SKB TR 97-09, Swedish Nuclear Fuel and Waste Management Company, Stockholm.

## APPENDIX A      DERIVATION OF THE RESIDENCE TIME FOR PERIODIC TOPOGRAPHY

An incompressible liquid flows two-dimensionally through a permeable rock that fills a half space. The conductivity and porosity of the rock are  $K(z)$  and  $n$ , respectively. The equation of the free surface is  $z = \phi_s(x)$ . The amplitude of  $\phi_s$  is small in the sense that  $|d\phi_s/dx| \ll 1$ . The flux per unit area is called the velocity  $\bar{v}(x, z)$ . The mass conservation law and Darcy's law,

$$\nabla \cdot \bar{v} = 0$$

$$\bar{v} = -K(z)\nabla\phi$$

define the flow.  $K(z)$  is known.  $\phi(x, z)$  is the unknown hydraulic potential. The boundary condition at the free surface  $z = \phi_s$  is linearized, i.e. the condition is satisfied at  $z = 0$ . Thus the real domain  $R : \{-\infty < x < \infty, \phi_s \leq z < \infty\}$  is replaced by the fictitious domain  $R_f : \{-\infty < x < \infty, 0 \leq z < \infty\}$ . At infinite depth, the potential is undistributed. Thus the boundary conditions are

$$\phi(x, z = 0) = \phi_s(x)$$

$$\phi(x, z \rightarrow \infty) = 0,$$

where  $\phi_s(x)$  is either periodic, or vanishes for  $|x| \rightarrow \infty$ . In the latter case  $\phi(x)$  also vanishes from  $|x| \rightarrow \infty$ .

As mentioned previously, the conductivity decreases with increasing depth. Moreover, the shape of the free surface is characterized by a given length  $L$  and a given amplitude  $\phi_0 \ll L$  in agreement with the above assumptions. The length scale  $L$  is related to a "frequency"  $\omega$ , that is fictitious for the moment. Hence

$$\omega = \frac{2\pi}{L}$$

The above equations define the problem and yield the flow equation

$$\frac{\partial^2 \phi}{\partial x^2} + \frac{\partial^2 \phi}{\partial z^2} + \frac{1}{K} \frac{\partial K}{\partial x} \frac{\partial \phi}{\partial x} + \frac{1}{K} \frac{\partial K}{\partial z} \frac{\partial \phi}{\partial z} = 0$$

The exponential decay of conductivity with depth is the only relation that yields a closed solution of the flow equation. ( $z_0 \rightarrow \infty$  corresponds to constant conductivity). The terms that contain first-order derivatives are

$$\frac{1}{K} \frac{\partial K}{\partial x} = 0$$

$$\frac{1}{K} \frac{\partial K}{\partial z} = -\frac{1}{z_0}$$

It is convenient to introduce the following non-dimensional variables, including time, and parameters,

$$\hat{\phi} = \phi / \phi_0$$

$$\xi = \omega x \equiv 2\pi x / L$$

$$\zeta = \omega z \equiv 2\pi z / L$$

$$\hat{v} = \bar{v} / \phi_0 \omega K_0 \equiv \bar{v} L / 2\pi \phi_0 K_0$$

$$\tau = t / t_{ref} \equiv t \phi_0 \omega^2 K_0 \equiv 4\pi^2 t \phi_0 K_0 / L^2$$

$$\lambda = 1 / \omega z_0 \equiv L / 2\pi z_0$$

$$\hat{K}(\zeta) = K(z) / K_0 \equiv e^{-\lambda \zeta}$$

The above dimensional variables yield

$$\frac{\partial^2 \hat{\phi}}{\partial \xi^2} + \frac{\partial^2 \hat{\phi}}{\partial \zeta^2} - \lambda \frac{\partial \hat{\phi}}{\partial \zeta} = 0$$

$$\hat{\phi}(\xi, 0) = \hat{\phi}_s(\xi)$$

$$\hat{\phi}(\xi, \infty) = 0.$$

If the surface potential is simply periodic, i.e.  $\hat{\phi}_s(\xi) = \cos \xi$  the following simple approach

$$\hat{\phi}(\xi, \zeta) = \psi(\zeta) \cos \xi$$

The periodic boundary condition gives

$$\frac{d^2 \psi}{d\zeta^2} - \lambda \frac{d\psi}{d\zeta} - \psi = 0$$



$$\psi(0) = 1$$

$$\psi(\infty) = 0,$$

the solution of which is

$$\psi(\zeta) = e^{f(\lambda)\zeta}.$$

The auxiliary parameter

$$f(\lambda) = \frac{1}{2}(\lambda - \sqrt{\lambda^2 + 4}) < -1$$

describes the influence of the non homogeneous conductivity. The solution of the boundary value problem is

$$\hat{\phi}(\xi, \zeta) = e^{f(\lambda)\zeta} \cos \xi$$

The velocity  $\hat{v} = (v_\xi, v_\zeta)$  is

$$v_\xi = -\hat{K}(\zeta) \frac{\partial \hat{\phi}}{\partial \xi} = e^{(f(\lambda)-\lambda)\zeta} \sin \xi$$

$$v_\zeta = -\hat{K}(\zeta) \frac{\partial \hat{\phi}}{\partial \zeta} = -f(\lambda) e^{(f(\lambda)-\lambda)\zeta} \cos \xi$$

The absolute value of the velocity is

$$|\hat{v}| = e^{(f(\lambda)-\lambda)\zeta} \sqrt{\sin^2 \xi + f^2 \cos^2 \xi}.$$

Hence the greatest absolute value of the vertical velocity occurs below the "ridges" ( $\xi = 0$ ) or the "valleys" ( $\xi = \pi$ ), whereas the greatest absolute value of the horizontal velocity occurs "halfway" between a ridge and a "valley" ( $\xi = \pi/2$ ), i.e. where the slope is steepest.

The streamlines are given by

$$d\xi/v_\xi = d\zeta/v_\zeta$$

$$\zeta(\xi_0) = 0$$

The solution is

$$\zeta_s = -f(\lambda) \ln \frac{\sin \xi}{\sin \xi_0},$$

where  $0 \leq \xi_0 \leq \pi/2$  and  $\xi_0 \leq \xi \leq \pi - \xi_0$ . Hence a streamline is uniquely determined by  $\xi_0$ .

The velocity and the streamlines offer a possibility of calculating the dimensionless time it takes for a fluid particle to travel between points 1 and 2, along a streamline. If  $s$  is the dimensionless natural coordinate, it follows that

$$d\tau = \frac{ds}{|\hat{v}|},$$

where

$$ds = \sqrt{(d\xi)^2 + (d\zeta)^2} = \sqrt{1 + f^2 \cot^2 \xi} d\xi.$$

Then

$$\tau_2 - \tau_1 = \int_{\xi_1}^{\xi_2} \frac{d\xi}{e^{\zeta(\xi)(f-\lambda)} \sin \xi}$$

where  $\zeta_s(\xi)$  is given by (21) and the coordinates of the points 1 and 2 that are  $(\xi_1, \zeta_1)$  and  $(\xi_2, \zeta_2)$  respectively. If the coordinates of the repository are  $(\xi_r, \zeta_r)$ , the streamline that passes through the repository satisfies

$$\zeta_r = -f(\lambda) \ln \frac{\sin \xi_r}{\sin \xi_0},$$

which defines

$$\sin \xi_0 = e^{\zeta_r/f} \sin \xi_r.$$

If point 1 is the location of the repository and point 2 is located at the free surface, i.e.  $\xi_1 = \xi_r$  and  $\xi_2 = \pi - \xi_0$ , the travel time is called the residence time

$$\hat{T} = \int_{\xi_r}^{\pi - \xi_0} \frac{d\xi}{e^{(f-\lambda)\zeta(\xi)} \sin \xi}$$

If the repository is located below the bottom of a valley, the streamline is vertical and formulae are not valid. At the vertical streamline  $\xi = \xi_r = \xi_0 = \pi$  and  $ds = -d\zeta$ . The horizontal component of the velocity is equal to zero and

$$|\hat{v}| = f e^{(f-\lambda)\zeta} \quad ; \quad \xi_r = \pi,$$

which leads to

$$\hat{T} = \frac{1}{f} \int_0^{\zeta_r} e^{-(f-\lambda)\zeta} d\zeta = \frac{1 - e^{\zeta_r(\lambda-f)}}{f(\lambda-f)} \quad ; \quad \xi_r = \pi.$$

If the repository is located at very large depth,

$$\lim_{\zeta_r \rightarrow \infty} \hat{T} = -\frac{e^{(\lambda-f)\zeta_r}}{f(\lambda-f)} \rightarrow \infty \quad ; \quad \xi_r = \pi.$$

Two extreme cases are practically important and simple to analyze.

1.  $\lambda \ll 1$

$\lambda \rightarrow 0$  corresponds to the trivial solution for  $K(z) \equiv K_0$ . Then  $f \approx -1$  and

$f - \lambda \approx -1$ . The velocity is

$$v_\xi = e^{-\zeta} \sin \xi$$

$$v_\zeta = e^{-\zeta} \cos \xi$$

$$|\hat{v}| = e^{-\zeta},$$

and the streamline through the repository is defined by  $\xi_0 = e^{-\zeta_r} \sin \xi_r$ . The

equation of the streamline is

$$\zeta_s = \zeta_r + \ln \frac{\sin \xi}{\sin \xi_r}.$$

The absolute value of the velocity is thus independent of  $\xi$ , but decreases exponentially with the depth. The time it takes for a fluid particle to travel between points 1 and 2 is

$$\tau_2 - \tau_1 = \frac{\xi_2 - \xi_1}{\sin \xi_0}$$

and the residence time

$$\hat{T} = \frac{e^{\xi_r} (\pi - \arcsin(e^{-\xi_r} \sin \xi_r))}{\sin \xi_r} \quad \xi_r \neq \begin{cases} 0 \\ \pi \end{cases}.$$

If the repository is located exactly below a ridge or a valley, the residence time is

$$\hat{T} = \begin{cases} \infty & \xi_r = 0 \\ e^{\xi_r} - 1 & \xi_r = \pi \end{cases}$$

Not unexpectedly, the shortest residence time occurs if  $\xi_r = \pi$ , i.e. the repository is located below a valley.

## 2. $\lambda \gg 1$

$\lambda \rightarrow \infty$  corresponds to a boundary layer solution, since the second order derivatives in the flow equation vanish. The auxiliary parameters are  $f \approx -1/\lambda$  and  $f - \lambda \approx -\lambda$ . The velocity is

$$v_\xi = e^{-\lambda \xi} \sin \xi$$

$$v_\zeta = \frac{1}{\lambda} e^{-\lambda \zeta} \cos \zeta \approx 0$$

$$|\hat{v}| = e^{-\lambda \zeta} \sin \zeta,$$

and the streamline is defined by  $\xi_0 = e^{-\lambda \zeta_r} \sin \zeta_r$ . The equation of the streamline is

$$\zeta_s = \frac{1}{\lambda} \ln \frac{\sin \xi}{\sin \xi_0}$$

The travel time between two points, 1 and 2, is

$$\tau_2 - \tau_1 = \frac{1}{\sin \xi_0} \ln \frac{\tan \xi_2 / 2}{\tan \xi_1 / 2}$$

The residence time is

$$\hat{T} = \frac{\pi - \xi_r - \arcsin(e^{-\lambda \zeta_r} \sin \xi_r)}{e^{-\lambda \zeta_r} \sin \xi_r} \quad \xi_r \neq \begin{cases} 0 \\ \pi \end{cases}$$

and

$$\hat{T} = \begin{cases} \infty & \xi_r = 0 \\ e^{\lambda \zeta_r} - 1 & \xi_r = \pi \end{cases},$$

in analogy with the previous case. Similarly the shortest residence time occurs if the repository is located below a valley.

The simplified formulae of the above extremes are summarized in Table A.1.

**Table A.1** Simplified formulae

	$v_\xi$	$v_\zeta$	$ \hat{v} $	$\hat{T}$
$\lambda \ll 1$ (short waves)	$e^{-\zeta} \sin \xi$	$e^{-\zeta} \cos \xi$	$e^{-\zeta}$	$\infty$ $\xi_r = 0$ $\frac{e^{\zeta_r} (\pi - \arcsin(e^{-\zeta_r} \sin \xi_r))}{\sin \xi_r}$ $0 < \xi_r < \pi$ $e^{\zeta_r} - 1$ $\xi_r = \pi$
$\lambda \gg 1$ (long waves)	$e^{-\lambda \zeta} \sin \xi$	0	$e^{-\lambda \zeta} \sin \zeta$	$\infty$ $\xi_r = 0$ $\frac{\pi - \zeta_r - \arcsin(e^{-\lambda \zeta_r} \sin \xi_r)}{e^{-\lambda \zeta_r} \sin \xi_r}$ $0 < \xi_r < \pi$ $e^{\lambda \zeta_r} - 1$ $\xi_r = \pi$

A comparison between the two extremes shows that increasing  $\lambda$  reduces the depth of the streamline by a factor of  $\lambda$ . This implies a *shorter* streamline, which might indicate that  $\hat{T}$  decreases with increasing  $\lambda$ . This is not the case since  $K$  decreases with increasing  $\lambda$ .

## APPENDIX B      DERIVATION OF CHARACTERISTIC WAVE LENGTHS OF THE TOPOGRAPHY

Possible periodicity of the topography can be identified using either of two methods, which are described below. The basis for all calculations are elevation data in GIS. As mentioned in the introduction, the elevation is given at the nodes of a quadratic mesh. The distance between the points is 500 m. The fact that the mesh is quadratic simplifies the calculations considerably. All numerical calculations which are described below have been performed with the aid of the standard code MATLAB.

### Fast Fourier transform

The most straight forward and commonly used frequency analysis is the fast Fourier transform, in the sequel called FFT.

Since the elevation  $y(k_1, k_2)$  is a function of two variables, the 2D discrete Fourier transform

$$Y(n_1, n_2) = \sum_{k_1=1}^{N_1} \sum_{k_2=1}^{N_2} y(k_1, k_2) e^{-2\pi i(n_1 k_1 / N_1 + n_2 k_2 / N_2)} \quad \begin{array}{l} n_1 = N_1 / 2 \dots N_1 / 2 - 1 \\ n_2 = N_2 / 2 \dots N_2 / 2 - 1 \end{array}$$

applies. An estimate of the power spectrum is then

$$\hat{\Phi}(n_1, n_2) = |Y(n_1, n_2)|^2.$$



The amplitude corresponding to a particular frequency is estimated from the FFT as

$$a = \frac{2|Y(n_1, n_2)|}{N_1 N_2}$$

Details on the derivation can be found in the textbook by Brigham (1988). Each Fourier coefficient corresponds to the continuous frequencies in each of the two coordinate directions.

$$\omega_1 = 2\pi n_1 / N_1 P_1$$

$$\omega_2 = 2\pi n_2 / N_2 P_2,$$

where  $P_1$  and  $P_2$  are the spatial sampling intervals. Equation (8) yields the corresponding wavelengths.

$$L_1 = N_1 P_1 / n_1$$

$$L_2 = N_2 P_2 / n_2.$$

The FFT gives a spectrum only in discrete frequency points. If any of  $n_i$ , is small, i.e.  $L_i \sim N_i P_i$  the resolution is poor. However, the resolution can be enhanced by the aid of so called zero-padding.

### **Autoregression**

Another common method, albeit somewhat more complicated, is autoregression called AR in the sequel. In contrast to the FFT, the AR gives the spectrum at any point. On the other hand, the AR does not give any information about the *amplitude* of the components.

According to the AR method, the elevation  $y(n_1, n_2)$  is written

$$y(n_1, n_2) = -\sum_{k_1} \sum_{k_2} a_{k_1, k_2} y(n_1 - k_1, n_2 - k_2) + e(n_1, n_2),$$

where  $e(n_1, n_2)$  is white noise, the mean value and variance of which are equal to zero and  $\mu$  respectively. The two-dimensional z-transform applied to this equation yields

$$Y(z_1, z_2) = \frac{1}{A(z_1, z_2)} E(z_1, z_2),$$

where the filter polynomial  $A(z_1, z_2)$  is given by

$$A(z_1, z_2) = 1 + \sum_{k_1} \sum_{k_2} a_{k_1, k_2} z_1^{-k_1} z_2^{-k_2}$$

The summation, i.e. the region of support  $S_{mn}$ , remains to be chosen. Here a non-symmetric half-plane has been used. Hence

$$S_{mn} = \{k_1, k_2 \mid k_1 = 0, 1 \leq k_2 \leq m; 1 \leq k_1 \leq n, -m \leq k_2 \leq m\},$$

where  $(m, n)$  is known as the model order. Estimates of  $\mu$  and  $a_{k_1, k_2}$  can be obtained by applying the least squares method to the elevation data. An estimate of the spectrum in this case is

$$\hat{\Phi}(\omega_1, \omega_2) = \frac{\hat{\mu}}{|\hat{A}(e^{i\omega_1}, e^{i\omega_2})|^2}$$

Just as for the FFT, the dominating length scale are

$$L_1 = 2\pi P_1 / \omega_1$$

$$L_2 = 2\pi P_2 / \omega_2.$$